ISLAMIC AZAD UNIVERSITY

MASHHAD BRANCH

Faculty of Engineering

Thesis for receiving (M.SC) degree on Metallurgy and Ceramic Engineering

Subject:

Synthesis Nono Calcium Carbonate from Waste Gypsum

Supervisor:

Ebrahim Zohourvahid-Karimi Ph.D.

By:

2022

In The Name of God

Gratitude and Acknowledgments:

Dedication to him who taught me to learn

Dear Professor, Ebrahim Zohourvahid-Karimi Ph.D.

Contents:

Image title:

Table title:

Chapter One: General Investigation

1-1 Introduction

Calcium hydroxide is a mineral substance with the chemical formula Ca(OH)2 and one of the substances that has wide chemical, industrial, medical and construction applications. Among the uses of this substance, we can mention bleaching sugar purification, water purification, pollution control, protection of wooden works in historical buildings and antibacterial properties during nerve extraction in dentistry. Calcium hydroxide nanoparticles are prepared by various methods, the most important of which are: sonochemistry, microemulsion, sedimentation in an organic medium and precipitation.

1-2 Problem Statement

Due to its distinct physical and chemical features, precipitated calcium carbonate finds widespread application across a variety of sectors [1]. It is the structure of a material, including its crystal type and morphology, that ultimately determines the substance's qualities [2]. Carbon materials, for instance, may exhibit varying characteristics depending on their form and morphology [3]. Consequently, the product's structure, which is crucial in the processing steps, is investigated. Calcium carbonate crystals come in three different varieties [4]. Among these are the spherical mineral vaterite and the fibrous calcium carbonate and rhombohedral calcite [5]. Because of its fibrous shape, calcium nanocarbonate finds use in sealing and friction materials [6]. Calcite and vaterite sell for considerably more than calcium nanocarbonate does on the market. So scientists have spent a lot of time figuring out how to mass-produce nano-sized calcium carbonate [7].

Carbonation, decomposition of calcium bicarbonate, hydrolysis of urea, double decomposition, etc. are now the primary ways of preparing nano calcium carbonate [8]. Pure materials or natural minerals make up the bulk of the raw materials utilised in these processes, and morphology can be modified with the help of chemical additions [9]. When gypsum is manufactured via a dry process, a solid waste known as gypsum waste is generated. Roughly eight to ten tonnes of trash may be generated during the manufacturing of one tonne of gypsum. Gypsum garbage primarily consists of amorphous calcium silicate. Because of this, gypsum waste contains a lot of calcium and is relatively active chemically.

Therefore, it is a good material for the production of precipitated calcium carbonate. In Iran, about 80,000 tons of gypsum waste are produced annually, which theoretically can produce 7-10 mg of calcium carbonate. At present, waste is mainly used in the production of baked bricks, glass ceramics and concrete. So far, no reports have been reported on the use of gypsum waste for the production of nano calcium carbonate.

Studies conducted in the laboratory show that a compound composed of CaCO3, calcite, and calcium nanocarbonate may be produced with relative ease [10]. High-purity calcium nanocarbonate is produced by using gypsum waste as a raw material under mild conditions (low temperature and natural pressure) and without the use of any chemicals [11]. Calcium nanocarbonate may be economically prepared using gypsum waste, which also allows for the realisation of the utilisation of waste resources [12]. This investigation comprehensively explored the impact of experimental parameters on the crystal phase and shape of the products, including reaction temperature, Ca2+ concentration, ammonia quantity, carbon dioxide velocity, and time. At the same time, the entire production process was evaluated, and it was theorised that by-product recovery could help bring down production costs.

1-3 The Importance and Necessity of Conducting Research

Considering the annual production of huge amounts of gypsum waste and the continuous increase of CO2 emission in the atmosphere, it is necessary to find attractive approaches to solve these two environmental problems [13]. Investigations have shown that the production of calcium carbonate (CaCO3) from gypsum waste is accompanied by the thermal reduction of the waste to calcium sulfide (CaS), and then, aqueous carbonation produces low grade carbonate products (eg <90% as CaCO3) [14].

According to the statistics of 2019, about 8000 thousand tons of lime waste is produced in the country every year (estimates up to one million tons have been reported). One of the problems of these factories in the process of sugar production is dealing with gypsum waste. This wet waste is mainly composed of calcium carbonate along with organic matter, which when exposed to air in the open environment, causes unpleasant odor and environmental problems.

Therefore, in order to solve this environmental problem, recycling and processing of this waste is investigated. The gypsum waste delivered in almost dry form will be subjected to various tests to extract calcium carbonate and also calcium oxide nanoparticles. After designing and conducting

various tests, two pure calcium carbonate products and calcium oxide nanoparticles are produced with very good quality.

1-4 Research Objectives

1-4-1 The Main Objective

- Synthesis of nano calcium carbonate from gypsum waste

1-4-2 The Sub-Objectives

- Investigating methods of calcium nanocarbonate synthesis from gypsum waste
- Investigating the efficiency of calcium nanocarbonate synthesis methods from gypsum waste

1-5 Research Questions

- What are the synthesis methods of nano calcium carbonate from gypsum waste?
- What is the efficiency of calcium nanocarbonate synthesis methods from gypsum waste?

1-6 The General Structure of the Thesis

The research has five chapters as follows:

The first chapter 1: In this chapter, while reviewing the generalities of the research, the topic, the importance and necessity of conducting the research, the goals and hypotheses of the research have been discussed.

The second chapter: This chapter is allocated to a review of the research literature in order to achieve a general and comprehensive understanding of the research issue.

The third chapter: The purpose of this chapter is to describe the research method in more detail.

The fourth chapter: In the fourth chapter, firstly, all the necessary data were collected and then the analysis of these data was done.

The fifth chapter: The final chapter of this research has ended by presenting the results of the data analysis of the previous chapters as well as practical suggestions for future researches.

Chapter Two: Theoretical Literature and Research Background

2-1 Introduction

Calcium carbonate is one of the most common and widely used minerals as a filler. The ultra-fine or nano-sized particles of this material are economical and are very useful for use in various industries such as rubber, plastic, paint, paper, ink and food.

2-2 Precipitated Calcium Carbonate

Precipitated calcium carbonate (PCC) as a filler has wide industrial uses such as papermaking, coloring, plasticizing, pharmaceuticals, cosmetics, etc. [15, 16]. PCC filler can be synthesized through chemical methods such as precipitation of solutions (liquid-liquid and solid-liquid processes) or hydrated lime carbonation (liquid-gas and solid-liquid-gas processes). From the point of view of production in the factory, the carbonization process is known as the most economical industrial method of PCC production [17]; Because by transferring lime instead of PCC to the paper factory and also by using carbon dioxide gas from the gas flow from the furnace or the power supply unit of the factory, it is possible to save 40% per ton of PCC produced [15 and 18]. In this method, first, limestone is burned in order to prepare calcium oxide at a temperature of about 1000 degrees Celsius (reaction number 1). Then, by mixing calcium oxide with water, calcium hydroxide is formed (reaction number 2). Finally, the resulting calcium hydroxide becomes carbonized using carbon dioxide gas (reaction number 3).

$$CaCO3 \text{ -» } Ca0 + CO2$$

$$Ca0 + H2O \text{ - »} Ca(OH)2$$

$$Ca(OH)2 + CO2 \text{ -» } CaCO3 + H2O$$

One of the advantages of PCC is the possibility of adjusting and engineering its characteristics (such as particle size, morphology, surface chemistry, polymorph, etc.) through controlling process parameters or using additives [19]. Polymorphs of calcium carbonate are divided into three anhydrous forms (calcite, aragonite and vaterite), 2 hydrated crystalline forms (monohydrate and hexahydrate calcite) and calcium carbonate without regular form. Hydrated and irregular forms are relatively unstable and can easily transform into calcite, aragonite or vaterite. Calcium carbonate crystals can be described as solid particles with very regular atoms and a three-dimensional repeating structure, whose polymorph type is influenced by the atomic order of the

repeating network structure. Polymorphs of calcite, aragonite, and vaterite are usually synthesized in relatively cubic, needle-shaped, and spherical polymorphs, respectively [15, 20].

Fillers are used in the paper industry to achieve different goals, such as reducing the cost of production and improving the properties of the final product, such as surface smoothness, bulk, air resistance, printability, and light scattering coefficient; but the use of coarse fillers with sharp angles and many impurities causes many problems such as surface roughness and high friction in the process of paper production and conversion. Therefore, the introduction of cationic PCC nanoparticles with hydrogen bonding capability and high purity to the paper industry is a very desirable thing that will reduce the disadvantages of using mineral fillers in paper products. So far, the effect of using different water-soluble additives such as starch, chitosan and their derivatives as PCC modifiers has been investigated by many researchers [21-23]. Kuusisto and Meloney (2015) investigated the effect of using starch and carboxy-methyl cellulose on the synthesis of precipitated calcium carbonate and the results showed that the crystallization of particles is affected by process parameters, type and amount of added polymer [24]. Yang et al. (2013) reported that using a mixture of cationic starch and carboxymethyl cellulose can improve the binding of starch to the filler, and in terms of paper properties (such as tensile strength, brightness and opacity), the use of modified filler with a mixture of cationic starch and carboxy-methyl cellulose resulted in the creation of paper with better characteristics compared to papers containing precipitated calcium carbonate modified with cationic starch or papers containing precipitated calcium carbonate modified with carboxymethyl cellulose[25]. Antunes et al. (2008) investigated the potential of various cationic polyacrylamides as a preservative aid in papermaking, and introduced cationic polyacrylamide with medium charge density as the optimal polymer to increase durability due to less water drainage time and longer filler durability [26]. Zhao et al. (2005) modified industrial PCC with corn and potato starches and reported that papers containing modified fillers had better tensile strength, tear resistance, and folding resistance compared to the testifier sample. In addition, they reported that by using the method of mixing, draining, baking, grinding and finally separating the modified particles, it is possible to increase the unmodified starch to PCC particles up to 12% [19].

The investigations carried out by the authors show that so far little research has been done in the direction of using the simultaneous modification method with synthesis for the production of PCC. In addition, in the conducted searches, no research was found in the direction of using this method

with the carbonization process to produce cationic PCC filler. The interaction between modified PCC particles with unmodified starches (which are largely non-anionic) and anionic cellulose fibers is relatively limited [27 and 28].

Calcium titanate (CaTiO3: CTO) is one of the most important ferroelectric oxides from the perovskite family with the general formula ABO3 and from the family of crystalline solids, where A is a 2-capacitance metal and B is a 4-capacitance metal. At high temperature, it is paraelectric and has an ideal cubic perovskite structure with space group Pm3m, and at room temperature it is ferroelectric and has an orthorhombic structure with space group Pnma [29]. The change from orthorhombic to cubic phase takes place in two stages: The transition from the orthorhombic Pnma phase to the tetragonal phase 14/mcm will occur in the temperature range of 1373 to 1423 K and the transition from the tetragonal phase 14/mcm to the cubic Pm3m will occur at the temperature of 1523 ± 10 K [30]. Calcium titanate has a special place in various sciences, including material science, geology, chemistry and physics, due to its unusual dielectric and magnetic properties and its unique electrical properties and also the phase changer at different temperatures which can strongly affect the chemical and physical properties of this compound. Calcium titanate is used as a ceramic material in many electronic devices. This material has a high corrosion resistance against caustic solutions (vapours of alkaline materials). Also, this material has a high dielectric constant and low dielectric loss, and these characteristics make it possible to use CaTiO3 in microwave dielectric applications as a resonator (amplifier) and a capacitive filter [3-4-3]. Calcium titanate has been widely used to modify the structure of many materials including PbTiO3 and BaTiO3 in order to adjust their properties for different applications. One of the most famous applications of this compound is its use in missile tracking and also the conversion of electrical energy into mechanical energy and vice versa [37].

In the medical field, it has a significant application for the simulation of body fluid organs, and this ceramic material can be used to increase the resistance of artificial body parts. In addition, in the field of biomaterials, it is used to increase the adhesion of hydroxyapatite coatings under the titanium layer [38].

Mechanical alloying is described as a process in which a mixture of powders are ground together. Various parameters in this process affect the final structure of the product, which has led to the complexity of this process. During high-energy grinding, the particles undergo expansion, cold boiling, fracture and re-boiling [37]. The change of the plastic shape of the powder particles as a

result of impacts leads to their hard work and failure. After grinding for a certain period of time and reaching an equilibrium state between the boiling speed (leading to an increase in the average particle size) and the fracture speed (leading to a decrease in the average particle size), a steady state equilibrium is established [38]. From this stage, each particle has all the primary components, according to the ratio in which they are mixed, and the particles reach maximum hardness due to the accumulation of strain energy [39]. At this stage, the distribution of particle size is small. In the grinding process, due to the drastic change in the shape of the particles, the conditions for the penetration of the dissolved elements in the field are prepared. This process includes 3 systems including: 1) soft-soft, 2) soft-crisp and 3) crisp-crisp [40].

The best mixture is a soft-soft mixture. In the soft-crisp mixture, alloying depends not only on the fineness of the crisp particles for easy penetration, but also on the ability to dissolve solids in the composition of the soft phase network. However, if the crisp-crisp system is used in this process, due to the absence of soft compounds and as a result of reducing the amount of cold welding, it is unlikely in some cases of alloying. For the same reason, a higher Ball-to-Powder Ratio (BPR), higher speed, and as a result, a higher amount of energy input to the powder mixture is required for alloying [41-43]. In this system, the brittle compounds are continuously crushed during grinding, but in very small sizes, they behave like hammer-eating metals and there is no possibility of their becoming smaller [44]. In this system, the harder (more brittle) composition is crushed and it is placed in the softer (less brittle) composition. In this case, due to the greater penetration distance, more energy must be applied to the powder mixture. This energy can be provided either by the things that were mentioned before or by applying thermal processes. As it was stated, in this process, due to the drastic change in the shape of the plastic, the density of defects will increase, which will lead to the speed of penetration into the process. From the side of the particles becoming smaller and as a result of the reduction in the penetration distance (due to the reduction of the microstructure), the temperature of the reaction can be greatly reduced, so that otherwise, the reaction will not burn at room temperature [4-5-8]. Depending on the grinding conditions, two completely different reaction kinetics are possible:

- It is possible that during each hit the reaction is limited to a small volume, which results in a gradual transformation.
- If the reaction enthalpy is high enough, a self-progressing combustion reaction can start. In this case, the beginning of the combustion reaction will require a critical time. In this

case, if the particles of the powder mixture are both hard, fragile and crispy, due to the lack of density or partial density between the particles, combustion will take place slowly and the reaction will be slow. Many reactions are investigated both in the SHS (Self Propagating High Temperature Synthesis) system and in another system called mechanochemical MSR (Mechanically Induced Self Sustaining Reaction). Some of these self-extended reactions are independent of whether the reaction is initiated by grinding (MSR) or local heating (SHS) [49-51]. In general, the reactions considered in the SHS system are considered in the MSR system. In some reactions, mechanical activation is done before the SHS process, which is effective on the combustion speed and uniformity of the product. Combining these methods has created a connection between these two processes. In order to reduce the combustion time and temperature, the amount of BPR can be increased. On the other hand, in the case of using a small abrasive agent, it leads to no combustion reaction, and the occurrence of a combustion reaction depends on the use of large pellets [52-54]. To check whether the reaction is done gradually or self-combustion, it is necessary to determine the adiabatic temperature (Tad) of the reaction. The adiabatic temperature of the reaction can be calculated from relation 1:

$$(1)\ \Delta H_r = \Sigma C^{s}_{p} (Tm - T_i) + \Sigma \Delta H_m + \Sigma C^{l}_{p} (T_{ad} - Tm)$$

In this relationship, ΔH r is the enthalpy change caused by the reaction, Csp is the equivalent heat capacity of the reaction products in the solid state, Tm is the melting temperature of the products, ΔH m is the latent heat of melting of the products, and Clp is the heat capacity of the products in the solid state. Of course, in relation 1, the second and third terms on the right side are entered when each of the products are melted. Of course, in case of evaporation of one of the factors present in the reaction, thermodynamic expressions related to the evaporation process will also be included in the equation. In general, for a reaction to be a self-expand reaction, the adiabatic temperature must be 1800 K [55].

Of course, instead of calculating the adiabatic temperature, its simpler relationship, i.e. the ratio of the heat of reaction to the heat capacity of the product phase at ambient temperature, can be used. In some cases, due to the use of low-energy grinding, the burning time is relatively long. On the other hand, in some of the systems that have high solid materials, the opposite of the above occurs, so that it is possible, for example, that some reactions with higher temperatures have longer

combustion times. In this case, the combustion time and temperature will depend on other features of the system, such as the hardness of the raw materials. Adiabatic temperature alone is not a sufficient condition to carry out self-progressing reactions. Calcium titanate is formed by heating a mixture of calcium oxide (CaO) with titanium dioxide (TiO2) at a temperature of 1650 K, but the problem of this process is that due to the fact that all the materials are in a stable state, the production of the mentioned composition in this way faces a problem among these problems, we can point out the non-uniformity of the sample, contamination of impurities, carrying out the process at high temperature, the presence of coarse particles with different sizes and non-uniform distribution [35-40].

2-3 Synthesis of Calcium Carbonate Particles

Among the methods used for the synthesis of calcium carbonate particles are biomimetic methods (biomimicry and CO2 bubble method). In the biomimetic process, the size, shape, and phase of calcium carbonate can be controlled by using organic compounds, and this process itself is divided into the categories of spontaneous precipitation reaction, slow carbonation reaction, and reverse emulsion method [56 and 57]. Another method of synthesis of precipitated calcium carbonate (PCC) is the use of a two-membrane system including an emulsion liquid membrane (ELM) and a decomposition membrane tube (DMT); During this process, Ca 2+ is through DMT. After completely draining the water of these two types of foam, they are in a special device (AEAC) containing cationic wetting agent alkyl polyhexyethylene ammonium chloride Na2CO3 and the other aqueous solution (AES) containing the anionic wetting agent alkyl polyhexyethylene alcohol sodium sulfate CaCl2 reacts inside the water-oil emulsion droplets [58]. In another process for the synthesis of calcium carbonate nanoparticles, they have used two types of foams that are separately stabilized by surface wetting agents (surfactants) that the first foam consisting of C03 aqueous solution penetrates and finally contacts each other designed with ionELM. Then Ca+2 is produced [59]. Also, flame synthesis has produced calcium carbonate nanoparticles with a size of 20-50 nm. In this process of spraying in the flame, the combustion of certain prestructure containing calcium leads to the production of amorphous or crystalline calcium carbonate particles depending on the conditions of the spray flow. Another method for the synthesis of calcium carbonate nanoparticles is the growth of intermediate polymer, that the product can have good biocompatibility and be used in medical work. CaCO3, which is trapped by the surfactant layers,

reacts in the thin boundaries between the foam bubbles, and CO nanoparticles, the use of a more chemical precipitating method is also common in the production of ultrafine calcium carbonate powder. But this method causes particles to agglomerate and as a result, the desired particle size cannot be achieved [60]. In addition, this method requires precise control of several variables such as the concentration of reactants, time, rotation speed, pH, etc., which determine the size, crystal structure, and morphology of the particles [61].

Recently, the mechanochemical process has been used for the synthesis of different nanoparticles. This synthesis method, which is used for transition metals and ceramics; includes the mechanical activation of solid-state nodal reaction. Mechanical grinding of precursor powders leads to the formation of nano-sized composite structures that react during milling or subsequent heat treatment, thus forming a mixture of nanocrystals of the expected phase in a salt field. The mechanochemical process is very suitable for the mass production of nanoparticles [62 and 63].

Stosser et al.[64] synthesized calcium hydroxide by sonochemical method. These researchers first put calcium acetate and sodium hydroxide under ultrasonic waves so that the reaction takes place. As a result of the reaction, a mixture of calcium hydroxide and calcium carbonate nanostructures was formed as an intermediate composition, and then as a result of drying at low temperature, calcium hydroxide nanoparticles were identified as the final product of the reaction. This method is not a suitable candidate for industrialization due to the need for a relatively expensive ultrasonic device. In addition, in this method, simultaneous control of all parameters has not been done by the researchers. Using microemulsions is one of the other ways of controlled synthesis of nanoparticles. In a research, Nani and Di [65] were able to produce calcium hydroxide nanoparticles with this method. In this research, microemulsions containing different concentrations of NaOH and 2CaCl solutions were used. The results of this work showed that it is possible to synthesize nanoparticles with an average size of 2-10 nm and the average size of the particles depends on the weight percentage of NaOH and 2CaCl. In this method, the produced product is prone to carbonation in carbon dioxide atmosphere and the most use of this method is for the synthesis of small CaCO3 particles. Another method of synthesizing calcium hydroxide is precipitation in an organic medium. Di and Salvadori in a research, dissolved calcium chloride dihydrate in constant temperature bath conditions. Then sodium hydroxide dissolved in water was added drop by drop to this solution. Next, the formed particles that have micron dimensions were separated from the solution under vacuum by hot refining. The high solubility of calcium

hydroxide in organic solvent compared to water has made the synthesis of this material difficult by this method. Also, the organic materials used stick to the particles and cause agglomeration of the particles. As a result, the final product is micron in size, which includes nano particles stuck together. Precipitation is a process in which a new solid material is created due to the imbalance of the liquid phase, and then the stages of growth and agglomeration of the solid phase are performed [66].

This process begins with the preparation of a uniform solution containing the desired cations. Then this solution is mixed with a suitable precipitating agent to settle the desired phase [67]. Precipitation method is a simple, cheap and efficient method for the synthesis of many materials in the industry. Various variables are effective in the synthesis of a material by precipitation method. The most important of these variables include temperature, PH; additive percentage, reaction time, stirring effect and organic solvent percentage. In order to synthesize calcium hydroxide in this way, Wilhemi et al. have reported that metal hydroxide precipitation using the corresponding salt is influenced by temperature and reaction time. Also, Yura et al. and Hamada et al. after synthesizing calcium hydroxide showed that the choice of organic solvent can affect the size and shape of the hydroxide particles obtained from the precipitation reaction [68].

2-4 Scanning Electron Microscopy

One of the most important aspects of nanostructures studies is the ability to make images of nanometer materials. Since visible light has a wavelength between 380-750 nm, light microscopes cannot be used to observe structures smaller than 100 nm. Therefore, in electron microscopes, by using electrons as a source of image formation, it is possible to image nanometer structures. Due to the low wavelength of the electron beam in electron microscopes, the magnification, depth of field and resolution of electron microscopes are several times that of optical microscopes. Investigating the microstructure of nanomaterials is one of the key parameters in studying and investigating their properties. Therefore, scientists are always looking for tools that can be used to observe and examine the microstructure of nanomaterials with good accuracy. Microscopic methods are methods that can be used to observe and examine the microstructure of matter. Microscopic methods based on light are not suitable for observing nanomaterials and do not have the necessary ability to observe materials in nano dimensions. Various microscopes such as scanning electron microscopy, transmission electron microscopy, atomic force microscopy and

scanning tunneling microscopy can be used to observe and examine nanomaterials. Scanning electron microscopy is an invaluable tool for characterizing nanostructures that can provide a range of different imaging modes and information on elemental composition and electronic structure with very high sensitivity for a single element [69]. A vacuum environment is needed to work with an electron microscopy. After the sample has been placed in the chamber, the vacuum inside the microscope column is brought to an appropriate level using the preexisting pumps. The electron beam is generated and focussed onto the sample using thin electromagnetic lenses after the necessary vacuum is reached. In fact, data is collected by scanning the electron beam across the sample. When an electron beam strikes a sample, it causes the generation of specific signals, which are then picked up by detectors and processed to yield the desired image or data. SEM microscope has six main components, which are: electron gun, electromagnetic lens, scanning system, detectors, image display system and vacuum system. Figure 1-2 shows the components of an SEM.

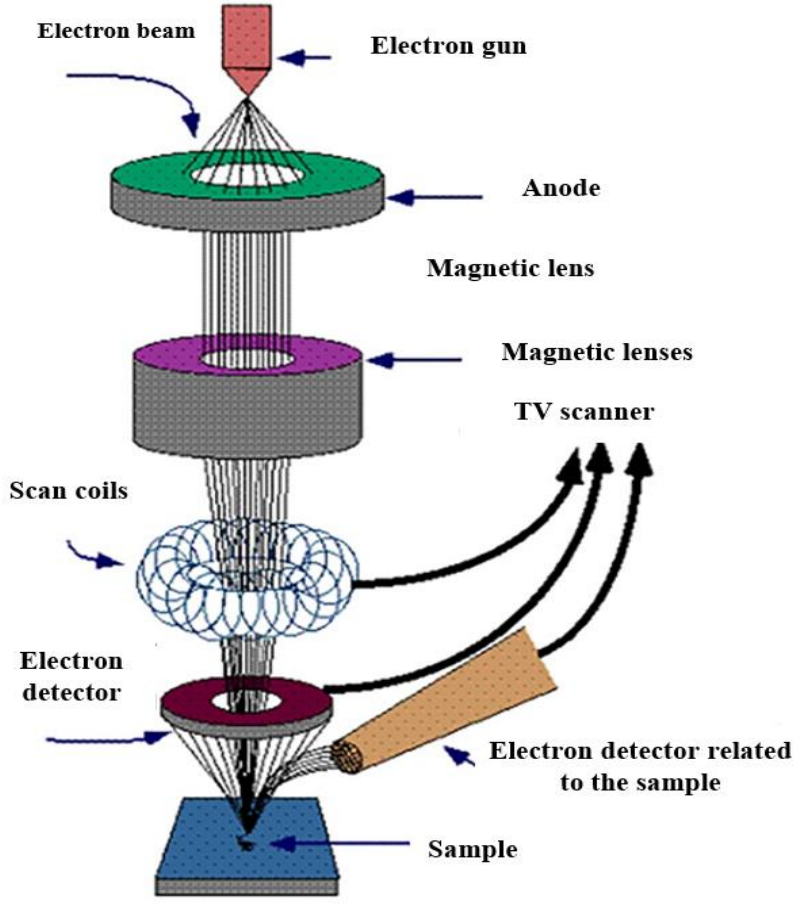

Figure 2-1 Schematic of a SEM scanning electron microscopy

2-4-1 Structural Design of SEM and its Components

Electrons exiting a cold FEG electron gun are merged into a probe smaller than 1 nm by the electrostatic exit gun lenses and objective lenses (L2) and magnetic concentrator (L1). The probe is scanned by two reflective coils [70] on the surface of the sample. Electrons exiting the sample enter the electron detectors. In the past, time-series signals were obtained for mapping by a cathode ray tube (CRT) [71]. But now a liquid crystal is used. This imaging system works basically like a television. Currently, single atoms can be imaged using modified SEMs. The magnification of SEM images is equal to the ratio of the screen size to the scanned area on the sample surface. The magnification in the SEM is varied by varying the current applied to the reflector coils. The resolution of SEM images is determined by the following factors:

- ✓ Intensity of scattered electrons and detection efficiency;
- ✓ the brightness of the electron gun and the aberrations of the focusing lenses (the object in the SEM), which determine the size of the electron probe;
- ✓ Lateral penetration of incident electrons that occurs inside the sample;
- ✓ The distance between scan lines on the screen [72].

Factor #3 refers to the worsening of seperation power by the lateral spread of the electron probe in the sample and the impact of the extended probe on components within the sample, for example, small clusters embedded in a crystal. Bright field (BF) SEM images are obtained using a detector (D) with a small acceptance angle. When an angular detector (D`) is used to collect electrons scattered at larger angles outside the direct beam disc, an angular dark field (ADF) SEM image intensity is obtained. Despite the lack of focus of the probe, the image of the atomic columns is always bright. This feature of ADF–SEM images is useful for identifying atomic columns in complex atomic structures where further interpretation of the observed image is possible. In high angle annular dark field (HAADF) SEM, the diffraction intensity is collected at higher angles [72]. The popularity of ADF-SEM imaging for the characterization of advanced materials is due to the non-rotation of the image with respect to the sample (alignment of the image and the sample) and thus the direct interpretation of the images [73]. HAADF–SEM images provide sample information that is sensitive to chemical composition [74] and provides quantitative chemical and structural information [75].

Important components in SEM are an electron gun to obtain a brighter electron beam and a series of lenses to create a small probe. In order to obtain a smaller and brighter electron probe, high-gloss FEG electron guns are needed [72]. The use of SEM is essential for the characterization of materials at the atomic scale, for example the characterization of defects, interfaces, or even in defective crystals. However, measurement of atomic column spacing or displacements is hampered in the presence of sample drift. During image acquisition, drift introduces distortions proportional to the drift velocity, which hinder accurate atomic structure measurements. Although modern SEM equipment is optimized to reduce vibration, air flow, and temperature fluctuations, some samples still drift [76].

2-4-2 Detectors

SEM's flexibility comes from the fact that it can pick up signals from a wide range of sources. Electrons with a specific amount of energy lost, secondary electrons, X-rays, and elastically scattered or scattered electrons can all be used in the same way as conventional TEMs. Under the sample, disc-shaped bright field (BF) and angular dark field (ADF) detectors measure the intensity of these electrons to form an image. Collection (sometimes simultaneously) of electrons conveying different forms of information is made possible by positioning the detector at various distances from the optical axis of the microscope, i.e. by employing various angular ranges in mutual space. The ADF detector has a tiny diameter, yet it mostly measures scattered electrons. Images captured at enormous diameters, in contrast, are recorded using high-angle, inhomogeneously scattered electrons (HAADF–SEM). In this example, the scattering potential of a given region of the sample determines the intensity at that location (atomic number contrast). Since the BF-TEM images include much of the information available in the direct beam, such as diffraction contrast and thickness-mass, the BF-SEM images will be consistent with them if the incident convergence half-angle is minimal. Information on phase contrast (PC) is also transmitted, as is well known [74].

It is highly desirable to image light elements during material characterization due to their scientific and technological significance in a wide range of materials (oxygen in superconductors, lithium in battery materials, hydrogen in hydrogen storage materials). Angular dark field (ADF) imaging in scanning electron microscopy (SEM) generates directly interpretable and powerful pictures for atomic-scale structural analysis, however the dominating thermal scattering contrast [75] occurs strongly in heavy elements. An angular detector placed in the bright field's outer region (towards the scattering zone) enables angular bright field (ABF) imaging [76], which permits simultaneous imaging of light and heavy elements with comparable contrast. Medium-angle bright-field (MaBF) imaging [77] is a similar technique that uses a detector on the axis of the disc with an outer angle of about half the angle of the diaphragm forming the probe (thus "medium") to reveal light and heavy materials with contrasting contrast and higher resolution. Color composite images combining MaBF and ADF data have been shown to improve visual interpretation [78, 79].

2-4-3 Z Contrast Imaging in SEM

Scattering is proportional to the Rutherford scatterer's cross section, hence most SEM images are created with a high angle annular dark field detector. The second power of Z2 depends on the atomic number of the scatterer centre, hence this subtype of imaging is known as atomic number contrast imaging [80]. While the electron probe scans the surface of the sample, high-angle scattering is collected on an annular detector and the output of a cloth is displayed on a television or computer screen, creating an atomic number contrast image. Each atom is assumed to scatter individually with a cross section dependent on the atomic number, therefore detecting the intensity scattered at high angles and integrating it across a large angular range effectively averages the correlated effects between atomic columns in the sample. This cross section generates a sharply peaked object function [81] at atomic sites. As the width of this objective function is quite narrow (about 0.1 angstrom), the spatial resolution is only constrained by the size of the microscope probe. Individual atomic columns can be lighted for a crystalline material along the zone axis, where the atomic distance is greater than the probe size. Scan the probe across the sample, and you'll get an atomic-resolution hybrid map, where the intensity is proportional to the average atomic number of the column's constituent atoms. Because the contrast in the image is not reversed by the shift in focus and thickness, the positions of the atoms may be established with great precision in the lab. The probe can be placed to capture electron energy drop spectra from specific locations inside the structure, allowing for a comprehensive spectral analysis to be performed in respect to the atomic scale image [82].

2-4-4 The Inability of Optical Microscopes to Observe Nanomaterials

If we want to detect a substance or object by the radiation of a wave, one point should be noted. Each wave can only detect objects or materials whose size is greater than or equal to its wavelength. As a result, with visible light, it is not possible to observe and examine objects or materials smaller than the visible wavelength. As you know, the visible wavelength is 380-750 nm. As a result, it is not possible to examine nanomaterials with dimensions less than 100 nm with visible light. For this purpose, one should look for waves with a wavelength less than 100 nm. In figure 2-2, the wavelength of a range of waves is displayed. At the bottom of this figure, each of the objects or materials that can be identified with each of the waves is also displayed [83].

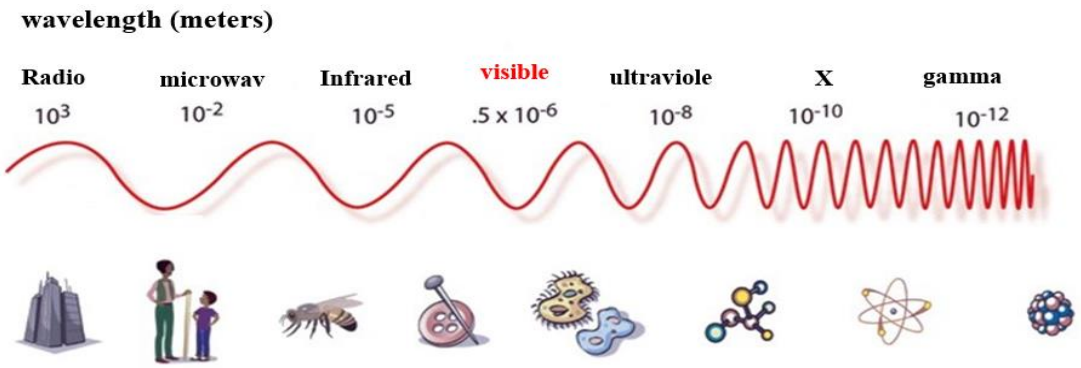

Figure 2-2 The wavelength of a range of waves and the things that can be recognized by each of them.

As you can see in Figure 2-2, visible light can be used to observe and examine objects that are larger than 750-380 nm in size. Electrons are usually used to observe and examine nanomaterials. Note that according to the concept of wave-particle duality, the electron can also show wave properties. The wavelength of the electron is less than the size of nanomaterials, and as a result, it is a suitable option for use in microscopes [83].

Figure 2-3 An image of a light microscope specimen

Electron microscopes were developed because of the limitations of optical microscopes. Using microscopic methods, high-magnification images of the material are obtained so that its details can be studied carefully. The resolution of microscopic images is determined according to the type of beam used. For example, resolution of about 1 μm or even 200 nm can be achieved using optical microscopes, and using electron, STM, AFM, and ion microscopes, high resolution from about one nanometer to a few angstroms is accessible. In this regard, the vertical and horizontal accuracy

of some of the most important microscopic methods are shown in Figure 4-2. As seen in Figure 4-2, many methods overlap, especially in the range of 10-100 nm. However, these methods do not necessarily produce images from the same part of the sample. For example, SEM and TEM both have a lot of overlap, but the former images the surface and the latter images the interior of the material [84].

In an optical microscope, it is possible to increase the magnification of the images by changing the surface curvature of the lenses (the degree of concavity and convexity) and their number, but due to the long wavelength of light, the images practically lose their clarity at magnifications above 2000. For example, to see the structure of organic cells, a magnification of 10,000 times is needed, which cannot be achieved by an optical microscope with visible wavelength [85].

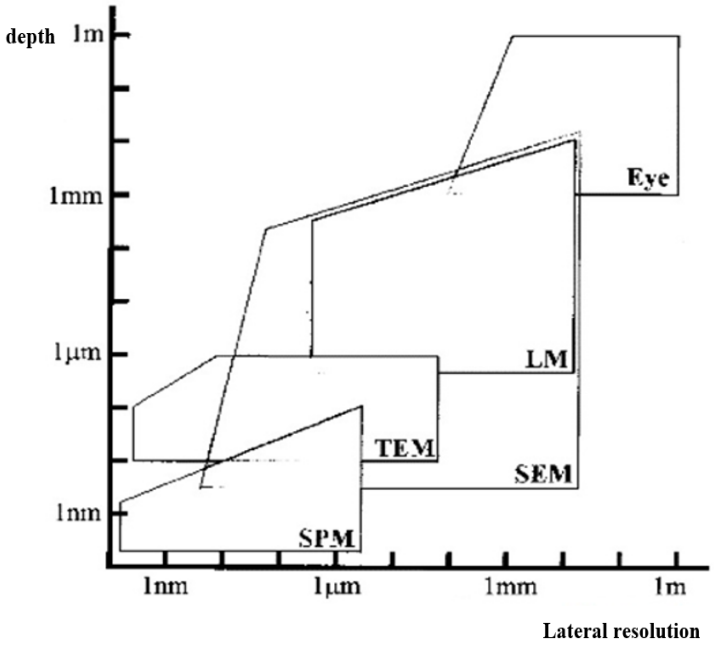

Figure 2-4 Vertical and horizontal resolution of different imaging methods

The interaction of the electron beam with the sample is fundamental to the functioning of the scanning electron microscope. Research can make use of the rays produced by this collision. The development of SEM made it possible for scientists to examine samples with greater clarity and convenience. Electron beam bombardment of a sample results in the emission of electrons and photons, which travel through the sample and are detected by detectors. As the beam moves across the sample, it generates a series of signals that the microscope uses to update the cross-sectional image of the sample surface in real time [86].

Therefore, the working mechanism of SEM is completely different from optical microscopes. At first, the main advantage of the SEM device was the preparation of microscopic images directly from solid samples with better clarity, resolution and focus compared to optical microscopes. But later, the executive and operational power of the device was developed and it was equipped with analysis methods, such as X-rays to determine the chemical composition. Figure 4-2 shows an example of a conventional SEM [85].

Figure 2-5 A picture of a SEM device

2-4-5 Characteristics of Image Quality

2-4-5-1 Resolution Power

Resolution is the smallest distance between two points that the microscope can distinguish separately. The lower the resolution, the more detail is shown in the microscope image. For this purpose, in SEM and TEM microscopes, the more concentrated the electron beam, the lower the resolution. Also, in AFM and STM microscopes, the smaller the size of the probe tip, the lower the resolution power [87]. Of course, the size of the probe tip should not be reduced so much that not enough signal is sent from the sample. The resolution power of microscopes is expressed by the following relationship:

$$r = \frac{0.61\lambda}{\mu \sin(\alpha)}$$

where λ is the wavelength of the imaging beam, μ is the refractive coefficient of the image medium, and α is the imaging angle. With the help of this relationship, it is possible to compare the resolution of optical and electron microscopes. The imaging angle in electron microscopes is much lower than optical microscopes, and most importantly, the wavelength of electron beams is much lower than visible light rays (the wavelength of visible light photons is 380 to 750 nm and the common wavelength in common electron microscopes is less than 0.06 nm). This value decreases with increasing electron microscope accelerator voltage. Due to the very large effect of the difference in the wavelength of light and electron beams, the effect of changes in the refractive coefficient will be insignificant. Therefore, the resolution power of an electron microscope is much better than that of an optical microscope. It should be noted that the resolving power is always larger than the diameter of the incoming electron beam. For example, in Figure 6-2, the resolution power of the image taken with the electron microscope is lower and the details are more and better known [87].

Figure 2-6 Comparison of resolution power in scanning electron microscopy and optical microscopy

2-4-5-2 Field Depth

Better depth of field means the possibility of distinguishing and recognizing details better and more accurately in images whose different components have different depths. For example, you can see in Figure 7-2 that the depth of field is much better in the electron microscope and you can easily distinguish the details of the image at different depths. The depth of field in SEMs is much

greater at lower magnifications. For example, the depth of field at magnifications below 20 is about 2 mm. In addition, at a fixed magnification, the depth of field of an SEM is more than 100 times the depth of field of an optical microscopy [88].

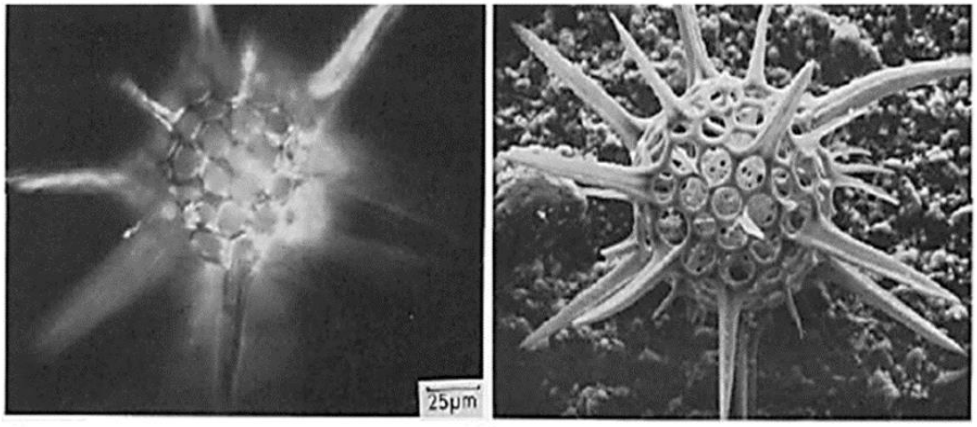

Figure 7-2 Comparison of the depth of field in the image of electron microscopy and light microscopy

2-4-5-3 Magnification

In optical microscopes, lenses are placed in the path of rays that are passed or reflected from the surface of the sample and by changing the angle of the beam movement and then changing the intersection of the rays, they lead to magnification. This is true for the objective lens in transmission electron microscopy, but not in SEM. A very important and interesting thing about the magnification mechanism in SEM is that the lenses only adjust the characteristics of the primary electron beam and do not affect the characteristics of the beams emitted from the sample. Therefore, it can be said that lenses do not have a direct effect on the magnification of SEM images. However, it should be remembered that the diameter and other characteristics of the rays emitted from the sample are influenced by the primary electron beam prepared by the lenses embedded in the optical column.

The magnification mechanism in the electron microscopy is actually the result of a geometric ratio and can be calculated based on the following equation:

$$M = \frac{L_{CRT-Raster}}{L_{Sample-Raster}}$$

where magnification is the ratio of the length of the CRT image line to the length of the image line on the sample (or the ratio of the side of the square under the effect of the beam (on the sample) to the square side of the CRT). Due to the fixed characteristics of CRT as a hardware factor, by

reducing the square size under the effect of the beam (which is called the image frame), the magnification can be increased. Therefore, the magnification in SEM is determined by the current of the x and y scanning coils.

For example, if the electron beam scans a surface of 10 x 10 square micrometers on the sample and the image on the CRT is 100 x 100 square millimeters, the linear magnification will be 10,000 times. Now, if we want to increase the linear magnification to 100,000 times, due to the hardware stability of the CRT dimensions, we must reduce the surface scanned by the electron beam to a square with sides of 0.1 micrometer. It is possible to use surface magnification instead of linear magnification and area ratio instead of length ratio [87].

2-4-6 Comparing Electron Microscopes with Optical Microscopes

Some important differences between light microscopes and electron microscopes are given below:

- Using electrons instead of light in electron microscopes
- Much higher resolution in electron microscopes due to the use of electrons that have a very short wavelength.
- Much higher magnification in electron microscopes
- Much greater depth of field in electron microscopes (about 300-500 times more)
- Optical microscope lenses are made of glass, but electron microscope lenses are electromagnetic lenses made of a copper coil.
- In light microscopes, the radiation source is located below the sample, but in electron microscopes, it is located above the sample (electron gun).
- Electron microscopes mostly work in vacuum (such as SEM and TEM), but light microscopes work in air or any other fluid.
- Electron microscopes are more expensive [89].

2-4-7 SEM Electron Microscope Applications

Many materials such as metals, alloys, magnetic materials, superconductors, semiconductors, ceramics, composites, bimetals, powders, ionic crystals, polymers, insulators, rubbers and plastics are used in studies.

The scanning electron microscope has many applications in nanotechnology, including measuring the size range of nanoparticles and investigating their morphology, investigating the structure of nanocomposites, the structure of nanotubes, the changes of nanostructures in different operations, nanofibers, nanostructure coatings, pharmaceutical nanostructures and biological samples on a nanoscale [89].

2-4-8 Advantages and Limitations of SEM Electron Microscopy

The following are the advantages of SEM electron microscope:

- The possibility of examining almost all types of conductive and non-conductive samples;
- No need for transparent samples;
- The possibility of imaging in three dimensions X, Y and Z;
- Ease of working with the device;
- the speed of working with the device;
- Requires little initial preparation for most samples.

Also, the SEM electron microscope has the following limitations:

- Expensive, large and requiring an environment free from electrical, magnetic and vibrational interference;
- the need for high vacuum in the system;
- low resolution, usually at more than a few tens of nanometers;
- The black and white images are due to the use of electron beam (however, in modern systems that are equipped with image analysis software, relatively colored images can be obtained by creating artificial colors (pseudo-color)) [89].

2-5 The Background of the Research

Source [6] presented a method to prepare nano calcium carbonate slurry using waste gypsum as a calcium source. This method includes the following steps: Add water in waste gypsum to prepare gypsum slurry, stir and mix ammonia water and gypsum slurry, feed carbon dioxide, stir the mixture until calcium sulfate in waste gypsum is completely converted to nano calcium. Carbonation, filtering and dispersion of filter cake in water to obtain nano calcium carbonate slurry. This method is simple and easy to operate, it is low cost and the decomposition temperature

of calcium carbonate is low. This invention further shows the nano calcium carbonate slurry prepared by the method and application of nano calcium carbonate slurry to prepare carbon dioxide absorbent based on calcium oxide and composite catalyst for reaction and absorption of methane vapor to produce hydrogen with modification. The prepared carbon dioxide adsorbent based on calcium oxide has good cycling stability and high absorption rate. The composite catalyst is used to produce methane steam hydrogen by reforming, so hydrogen with a purity of more than 90% can be produced.

Calcium carbonate precipitation synthesis was studied in source [7]. Precipitated calcium carbonate is essential to the survival of many companies, including those that produce paper, paint, adhesives/sealants, and plastics, due to the high demand for these products around the world (PCC). They're put to work as both reinforcements and fillers. Today, PCC is one of the world's leading manufacturers of plastics and papers. A variety of chemical and inorganic additives were utilised to synthesise distinct polymorphs of calcium carbonate, and their effects are discussed in this article. Optical characteristics, durability, smoothness, and ink absorption in paper manufacturing, as well as mechanical properties of plastic, can all be enhanced by using calcium carbonate precipitated fillers. The most efficient method for making PCC involves bubbling CO2 gas over a concentrated mixture of calcium hydroxide (Ca(OH)2) and/or calcium magnesium hydroxide (Ca Mg (OH)), both of which may be made in a laboratory. Substitute appropriate organic additions for the slurry. Different polymorphs of precipitated calcium carbonate have been synthesised using a wide range of organic and synthetic additives and reaction conditions. Different PCC polymorphs, including nano calcium carbonate, vaterite, and calcite, play important roles in the plastics and rubber sectors depending on their final application.

Source [8] investigated the synthesis of calcium carbonate nanoparticle deposition using membrane processes. In this article, calcium carbonate precipitation in different sizes using calcium ion concentration has been used as a controller. These calcium carbonate nanoparticles have been investigated at a higher temperature in order to determine their effects on the size of the emulsion particles. The experimental method used has been modeled using the Takayuki method and we have come to the conclusion that the oil-water emulsion has an unstable trend over time. Stabilizing the conditions at a constant pH creates suitable conditions for the formation of calcium carbonate nanoparticles. In order to change the concentration of the system, sodium nitrite is added to the reaction as a free ion.

In order to synthesise calcium carbonate, the process of desulfurizing gypsum in integrated reaction and separation equipment was studied in source [9]. Desulfurized gypsum is produced as a by-product when limestone and gypsum are desulfurized. The process of recycling gypsum that has been desulfurized involves mixing CaCO3 and (NH4)2SO4. In this work, we demonstrate the effectiveness of gypsum desulfurization by presenting integrated reaction and separation equipment. The nucleus's expansion and crystal formation were both monitored and managed via the use of additives and various mixing protocols. Additionally, the integrated machinery's separation mechanism and process parameters are designated. In addition, the properties of induced separation, as well as the movement and distribution in equipment, were evaluated using a computational fluid dynamics approach, including the examination of flow pathways and velocity profiles. We discovered that increasing the amount of reactants in the mixture improved the separation rates. The solid products have a low moisture content, and the efficiency of the solid-liquid separation degrades with increasing liquid velocity. Separation efficiencies of 83.83 percent and conversion rates from chemical reactions of 83.14 percent produce the best final products.

Chapter Three: Research Method

3-1 Research Method

The method of conducting this research is practical in terms of its purpose and descriptive and analytical in terms of implementation.

The raw material of waste is prepared in the country. In the prepared waste, the main chemical composition was CaO and SiO2, and some Fe2O3, P2O5 and Al2O3 are also present during the experimental investigation. The field investigation shows that the particles in the waste are amorphous in nature and the microstructure of the waste is granular.

For the purpose of the synthesis process, the waste is ground into a powder less than 150 micrometers. Other substances are used in the reaction such as CaCl2, HCl, NH4OH and 99.9% CO2.

The composition of gypsum waste and leaching product (weight percentage)

Material	**CaO**	**MgO**	**SiO_2**	**P_2O_5**	**Al_2O_3**	**Fe_2O_3**	**Others**
Yellow phosphorus slag	50.31	2.93	34.70	3.80	3.47	3.12	1.67
Leaching product	0.27	0.05	98.12	0.17	0.31	0.14	0.94

The whole preparation process is carried out according to the similar experiments in the previous study. During the experiments, the effect of the reaction conditions (temperature, Ca2 + concentration, ammonia amount, CO2 flow rate and time) on the preparation process of calcium carbonate nano is systematically discussed. The concentration of Ca2+ in the acid washing solution is considered one unit and we evaluate the change using distilled water and CaCl2.

Calcium carbonate nanoparticles are white powder, the average particle size (nanometers) is 15 to 40 nanometers. Its molecular formula is CaCO3. Calcium carbonate appears as a white, odorless powder or colorless crystals. Practically does not dissolve in water. It occurs widely in the rocks of the world. Calcium is found in minerals such as gypsum, plagioclase, dolomite, pyroxenes and garnets. In addition to various industrial applications as an alloying material, calcium is also an essential biological element found in bones, teeth, and shells. Calcium carbonate nanoparticles are synthesized through precipitation of calcium nitrate and saturated sodium carbonate solution.

3-2 The Method of Work Implementation

The conversion of gypsum waste into calcium carbonate particles has been done using a direct carbonation method, where the formation of calcium hydroxide and its conversion into calcium

carbonate particles occur simultaneously. The corresponding chemical reaction followed the following equation.

$$CaSO4 \cdot 2H2O + 2XOH + CO2 \rightarrow CaCO3 + X2SO4 + 3H2O \quad (1)$$

where X is either a sodium ion, a potassium ion, or an ammonium ion, depending on the solvent.

The following are the conditions for producing calcium carbonate from discarded gypsum:

5 grammes of gypsum, 1 litre per minute of carbon dioxide gas flow, 250 revolutions per minute of stirring, a temperature of 20 degrees Celsius, and a solid-to-liquid ratio of 1:20 (grammes per millilitre).

Both standard tube reactors and venturi reactors for carbonation were employed in the tests.

With the help of a Bandelin audiometer (SONOPULS HD 2070.2) set to 20 kHz, we were able to create ultrasonically with ease. TT13 titanium flat probe tip, diameter: 6 mm, length: 116 mm) is probed into the ultrasonic transducer.

To test how ultrasonic energy influences calcium carbonate particle formation, this setup was modified to work in a venturi tube carbonation reactor.

In this study, the reaction is carried out using (KOH), (NaOH), and a third alkaline source scenario (NH4OH). Further, the experiment required the use of three distinct kinds of reactors: (1) a standard tube reactor; (2) a venturi tube; and (3) an ultrasonic probe placed inside a venturi tube.

The amount of gypsum waste used ranged from 5 grammes to 50 grammes, with the first scenario using 10 grammes and the second two using 20 grammes and the third using 50 grammes.

3-3 The Ultrasonic Waves Method

The ultrasonic method is a relatively fast method that requires portable equipment. In addition, due to the use of sound waves and the absence of dangerous radiation, it is one of the safest and most common non-destructive methods for conducting periodic visits and determining residual stresses. This method has no limitations in terms of the type of material under investigation, and due to its greater penetration depth than X-rays, it is also used to measure stress in thick parts. The measurement of waste stresses with this method is based on the acoustoelastic properties of materials, based on which the propagation speed of ultrasonic waves in the material depends on

the existing stress. In this method, the higher the frequency of the generated wave, the lower its penetration depth, which is used to measure the stresses in the areas near the surface. In the ultrasonic method, the equipment used is placed next to each other in different ways; However, in all the mentioned arrangements, ultrasonic waves are produced by a device that is placed on the part. The generated waves, after propagating inside the part, are received using a receiver placed on another part of the sample. Finally, the residual stresses are calculated using the parameters obtained from the propagation of ultrasonic waves.

In the ultrasonic method, electrical energy is converted into pink energy by a device called a probe. The probe is made of a piezoelectric material that can convert electrical energy into sound waves and vice versa. Some natural or synthetic materials show piezoelectric properties.

Calcium carbonate is a natural piezoelectric and "barium titanate" is an artificial piezoelectric. When piezoelectric materials are exposed to an electric potential difference, they expand and contract and produce sound (mechanical) waves. Also, when the sound wave hits them, an electric potential difference is created at their two ends.

3-3-1 How Ultrasonic Devices Work

The ultrasonic device produces timed electrical pulses by the pulser and transmits them to the transducer through the coaxial cable. The probe converts electrical pulses into high-frequency sound waves (usually 1-10 MHZ) and transmits them to the part under test.

Sound waves are propagated in the piece at a certain speed and reflect upon hitting a new environment. The new environment means an environment whose density or the speed of sound propagation in it is different from the original environment. If the direction of the reflector is perpendicular to the direction of the sound, the reflected sound returns to the probe.

The piezoelectric crystal receives sound waves and converts them into electrical pulses. The electrical pulses are amplified by the amplifier and displayed as signals on the display screen (CRT). The operator interprets the signals according to their location, shape and height. By using calibration blocks with standard material, shape and dimensions, the ultrasonic device can be calibrated in order to accurately measure the distance traveled by the sound. According to the length of the sound traveled to the defect location, its exact depth can be calculated relative to the surface.

In general, the CRT screen contains two types of information. The location of the signal on the horizontal axis indicates the physical distance of the reflector to the transducer and the height of

the signal indicates the relative amount of sound energy reflected from the reflector. Of course, on the far left side of the CRT screen, there is always a signal called Main Bang.

The height of the signal on the CRT screen is an indicator of the size of the reflector. An experienced operator is able to determine the type, location and size of the discontinuity and accept or reject it according to the relevant code or standard.

3-4 Used Reactors

Figure 3-1 depicts the venturi tube and reactors that were most frequently utilised in this investigation. The test setup includes the following components: (1) a stabilisation tank, (2) a mechanical stirrer, (3) a pump for liquid circulation, (4) a venturi tube for mixing the solution and CO2 gas (this was just for the venturi tube reactor), (5) CO2 gas, (6) a CO2 flow metre, and (7) a data logger (pH metre, Gondo, PL-700AL) to monitor the pH of the solution in the reactor.

According to the results (Figure 3-1(c)-(d)), The solution in the venturi tube reactor had a Reynolds number of 106 X 1858., suggesting the presence of turbulent flow. In our earlier research, we laid out the foundational principles around which this apparatus operates. When the optimal pH was reached, carbonation was stopped by decreasing the CO2 flow in each experiment. After separating the solids from the liquids, the result was dried in an oven at 105 °C for four

hours. Finally, samples for various features were prepared.

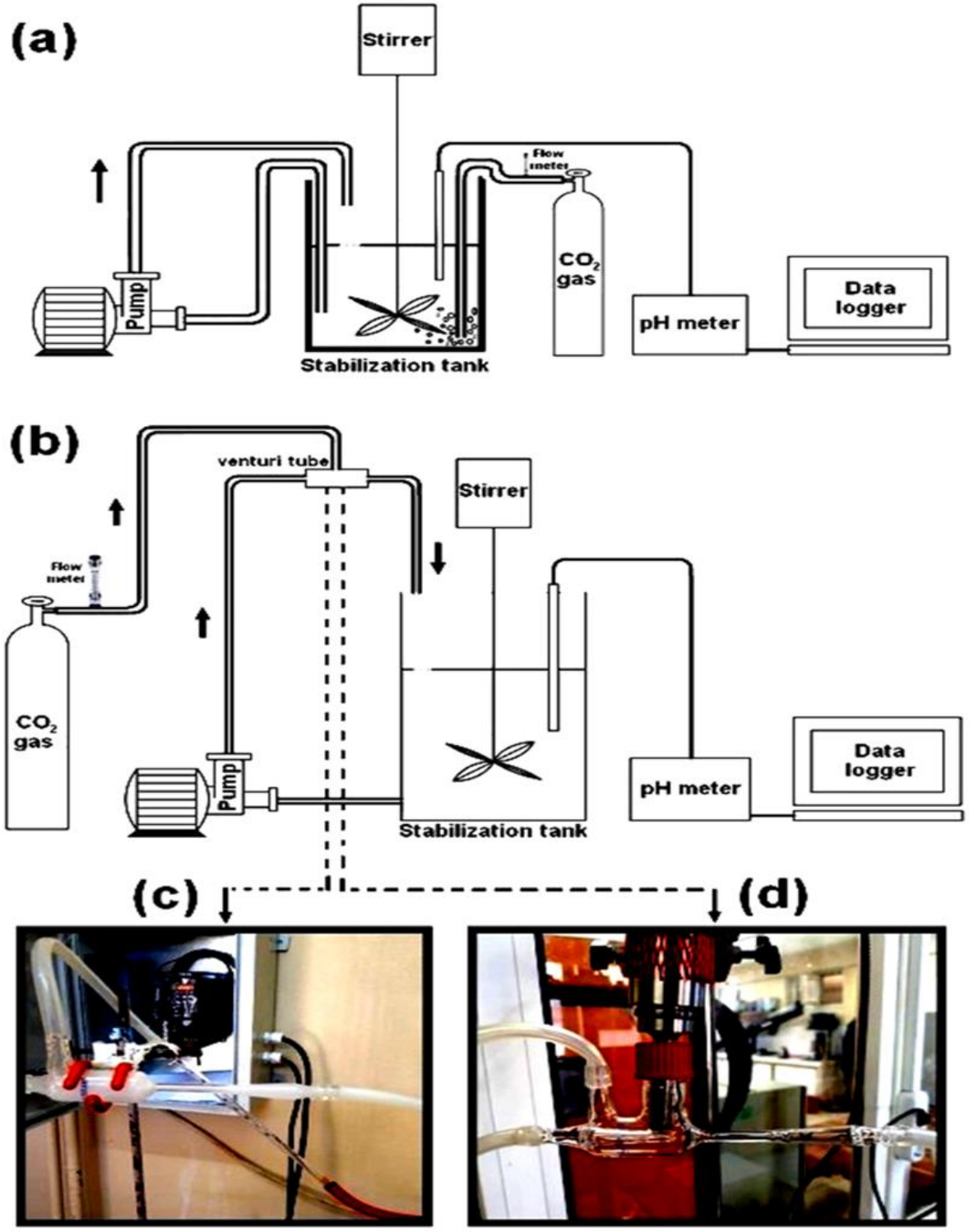

Figure 3-1 Equipment used in the experiments included (a) a standard reactor, (b) a reactor containing a venturi tube, (c) a venturi tube without an ultrasonic probe, and (d) a venturi tube equipped with a probe.

Chapter Four: Data Analysis

4-1 Introduction

Table 1 summarises the experimental conditions, along with their related symbols. Particles of calcium carbonate with the marking KV-UA were created with the use of a venturi tube for carbonation while adding K + ions. The application of ultrasonic energy following the production of calcium carbonate is denoted by UA.

UB in the test code indicates that the ultrasonic power was consumed before the CO2 flow was turned on. Extremely high frequencies were held constant at a 100% power range. The UA- and UB-code tests lasted 2 minutes, during ultrasonic energy with the highest amplitude was applied until the full reaction time had elapsed. Also, the UN claims that no ultrasonic power was employed throughout the experiment.

4-2 Test Characteristics

X-ray powder diffraction (XRD) with Cu-Ka radiation within the range of 2 15 -85 and a step size of 0.02 was used to analyse the phase parameters of the manufactured calcium carbonate particles. In order to determine what minerals were present, we ran a Rietveld analysis on the collected patterns using the PDXL and Diffrac-suite EVA programmes.

Calcium carbonate particle size distribution was evaluated using a Malvern Mastersizer and scanning electron microscopy (SEM; Gemini 300, Zeiss) was used to examine particle surface morphology (300H). Using an AFM (NanoSurf Flex Amf C3000) in static mode, the surface topology of carefully selected calcium carbonate particles was determined. We used Fourier transform infrared spectroscopy (Thermo Scientific Nicolet 6700) to examine the polymorphic development of certain calcium carbonate particles.

4-3 Results and Discussion

1- How ultrasonic treatment affects the reaction time needed to create calcium carbonate particles.

Calcium carbonate particle manufacturing conditions were tested through a series of tests. Carbonation causes a change in solution pH, which we observed using three distinct reactors (a standard tube, a venturi tube, and an ultrasonic probe used in the venturi tube) (see Figure 3). The interaction of Ca2+ ions with CO2 gas in the solution caused a drop in pH from 12 to 7.50. This indicates that the acidic solution is produced in the reactor when CO2 is dissolved as HCO3 ions.

By preventing the dissolution of the obtained calcium carbonate particles, by decreasing the pH to around 7.50, the rate of this process was slowed down. The pH of the solution is found to

decrease in a non-uniform pattern as a result of the cavitation that is noticed as a result of the ultrasonic power.

In this research, three alkaline source scenarios are used to implement the reaction including (KOH), (NaOH), (NH4OH). Also, in order to perform the experiment, three types of reactors were used, including 1- the type of conventional tube reactor, 2- the type of venturi tube and 3- the type of ultrasonic probe in the venturi tube.

Also, three different scenarios of using gypsum waste were used, including using 5 grams of gypsum waste, using 10 grams of gypsum waste, using 20 grams of gypsum waste and using 50 grams of gypsum waste.

Examining the conditions of postponement of scenarios

Table 4-1 Experimental conditions for the production of calcium carbonate from gypsum waste

Test number	Test code	Alkaline source Alkali	Type of reactor	Time to apply ultrasonic power
1	K-C-UN	KOH	Normal tube	Not applied
2	K-C-UA	KOH	Normal tube	After producing calcium carbonate
3	Na-C-UN	NaOH	Normal tube	Not applied
4	Na-C-UA	NaOH	Normal tube	After producing calcium carbonate
5	NH-C-UN	NH4OH	Normal tube	Not applied
6	NH-C-UA	NH_4OH	Normal tube	After producing calcium carbonate
7	K-V-UN	KOH	venturi tube	Not applied
8	K-V-UA	KOH	venturi tube	After producing calcium carbonate
9	Na-V-UN	NaOH	venturi tube	Not applied
10	Na-V-UA	NaOH	venturi tube	After producing calcium carbonate
11	NH-V-UN	NH4OH	venturi tube	Not applied
12	NH-V-UA	NH_4OH	venturi tube	After producing calcium carbonate
13	K-C-UB	KOH	Normal tube	Before producing calcium carbonate
14	Na-C-UB	NaOH	Normal tube	Before producing calcium carbonate

15	**NH-C-UB**	**NH_4OH**	**Normal tube**	**Before producing calcium carbonate**
16	**K-V-UB**	**KOH**	**venturi tube**	**Before producing calcium carbonate**
17	**Na-V-UB**	**NaOH**	**venturi tube**	**Before producing calcium carbonate**
18	**NH-V-UB**	**NH_4OH**	**venturi tube**	**Before producing calcium carbonate**
19	**K-C-US**	**KOH**	**Ultrasonic probe in venturi tube**	**During the production of calcium carbonate**
20	**Na-C-US**	**NaOH**	**Ultrasonic probe in venturi tube**	**During the production of calcium carbonate**
21	**NH-C-US**	**NH_4OH**	**Ultrasonic probe in venturi tube**	**During the production of calcium carbonate**
22	**K-V-US**	**KOH**	**Ultrasonic probe in venturi tube**	**During the production of calcium carbonate**
23	**Na-V-US**	**NaOH**	**Ultrasonic probe in venturi tube**	**During the production of calcium carbonate**
24	**NH-V-US**	**NH_4OH**	**Ultrasonic probe in venturi tube**	**During the production of calcium carbonate**

Na = NaOH, K = KOH, NH = NH4OH, V = venturi tube reactor, C = conventional reactor.

Amount of gypsum waste	KOH gypsum 5g waste	NaOH gypsum 5g waste	NH_4OH 5g gypsum waste	KOH gypsum 10g waste	NaOH gypsum 10g waste	NH_4OH gypsum 10g waste	KOH gypsum 20g waste	NaOH gypsum 20g waste	NH_4OH gypsum 20g waste	KOH gypsum 50g waste	NaOH 50g gypsum waste	NH_4OH 50g gypsum waste
Percentage of production of calcium carbonate with ordinary pipe	0.08	0.09	0.11	0.09	0.011	0.012	0.09	0.010	0.012	0.010	0.011	0.011
Venturi tube percentage production of calcium carbonate with	0.19	0.22	0.20	0.020	0.023	0.021	0.018	0.025	0.024	0.017	0.025	0.023
Percentage production of calcium carbonate with ultrasonic probe in venturi tube	0.23	0.28	0.28	0.025	0.032	0.028	0.024	0.030	0.031	0.029	0.032	0.028
The significance level	0.000	0.000	0.000	0.000	0.000	0.000	0.000	0.000	0.000	0.001	0.000	0.000
Correlation analysis of means (Pearson test)	0.026	0.011	0.016	0.006	0.036	0.041	0.039	0.047	0.041	0.034	0.049	0.027
Test result	positive and There are no differences	positive and There are no differences	positive and There are no differences	positive and There are no differences	positive and There are no differences	positive and There are no differences	positive and There are no differences	positive and There are no differences	positive and There are no differences	positive and There are no differences	positive and There are no differences	positive and There are no differences

The reaction time required to produce calcium carbonate particles

1- Calcium carbonate production scenario with a normal pipe with different amounts of 5, 10, 20 and 50 grams of plaster waste

2-

a. Before the production of calcium carbonate

b.

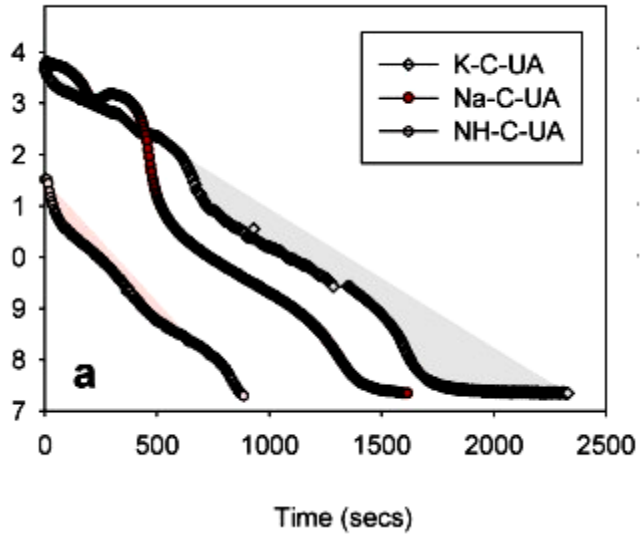

Figure 4-1 before the production of calcium carbonate

c. After the production of calcium carbonate

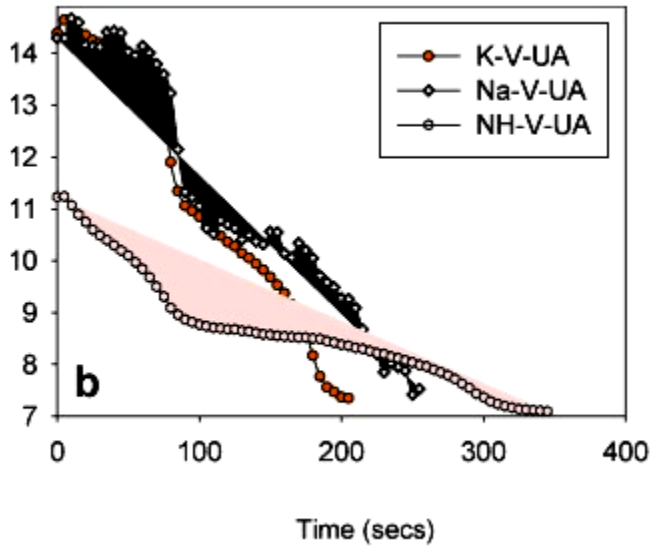

Figure 4-2 after calcium carbonate production

3- Calcium carbonate production scenario with venturi tube with different amounts of 5, 10, 20 and 50 grams of gypsum waste

a. Before producing calcium carbonate

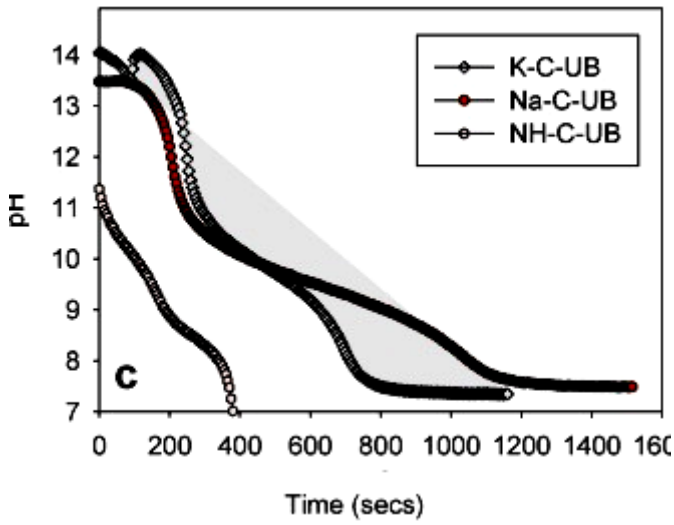

Figure 4-3 before calcium carbonate production

b. After the production of calcium carbonate

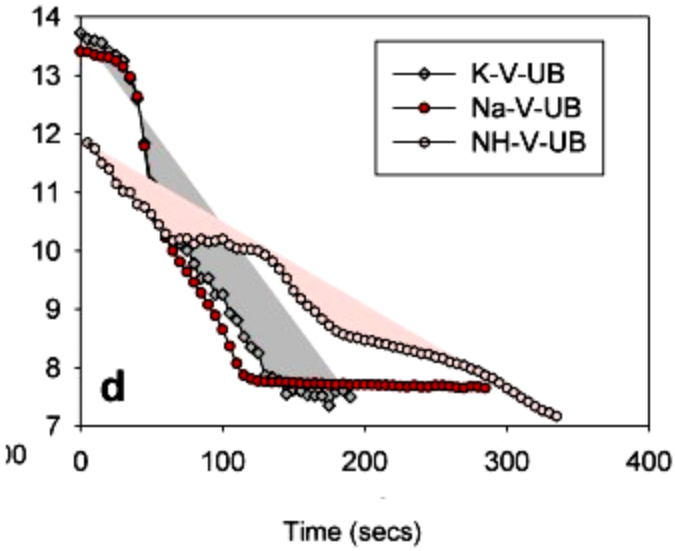

Figure 4-4 after calcium carbonate production

4- Scenario of calcium carbonate production with ultrasonic probe in venturi tube with different amounts of 5, 10, 20 and 50 grams of plaster waste

a. Before the production of calcium carbonate

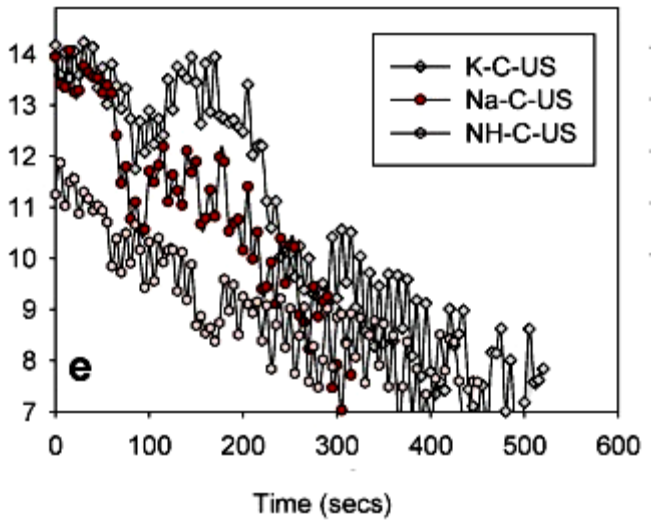

Figure 5-4 before calcium carbonate production

b. After the production of calcium carbonate

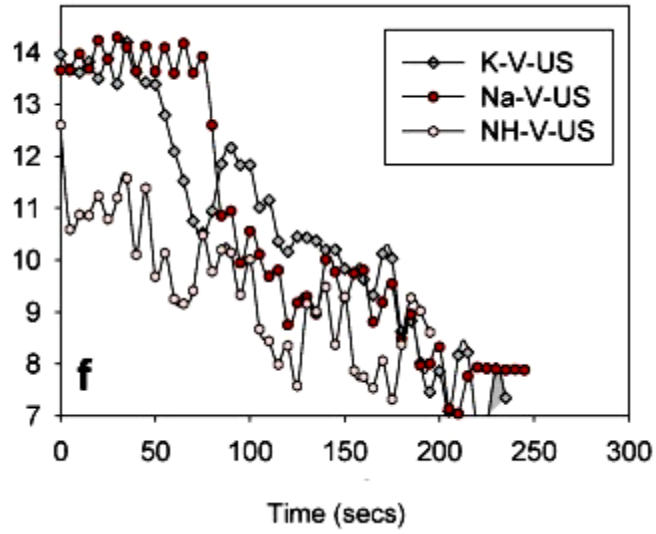

Figure 6-4 after calcium carbonate production

Figure 1-4 to Figure 4-6 changes in solution pH values in the presence of different alkaline sources: (a) C-UA, (b) V-UA, (c) C-UB, (d) V-UB, (e) C-US and (f) V-US.

Calcium carbonate particle production rates were shown to be very sensitive to carbonation reactor design. When compared to a standard carbonation reactor, the amount of time needed to

create calcium carbonate particles from gypsum waste through a venturi tube was significantly less. Time required to create calcium carbonate particles using Na + ions was 1435 s in the conventional reactor (Exp code: Na-C-UA, Figure 2(a)) and 250 s in the Venturi tube reactor (Exp code: Na-V-UA, Figure 2(b)). Similarly to our earlier investigation, this demonstrated that the venturi tube significantly influenced the calcium carbonate precipitation rate. Ultrasonic treatment in the venturi carbonation zone (test codes Na-C-UV and Na-V-US, Figure 2(e) and (f)) increases the nucleation rate of calcium carbonate particles, resulting in a quicker reaction.

Calcium carbonate particle nucleation rate (NR) was shown to be highly reaction-condition-dependent. The NR values determined using the pH curves in Figure 3 are presented in Table 2. The NR values of calcium carbonate in Na-C conditions are 20.28, 20.78, and 66.13 M/s. for the Na-C-UA, Na-C-UB, and Na-C-US, respectively.

Table 2-4 Nucleation rate (NR) of calcium carbonate and required reaction time in different production conditions.

Code	**NR (µM/s)**	**Reaction time(s). (s)**	**code**	**NR (µM/s)**	**Reaction time(s). (s)**	**Exp. Code**	**code**	**Reaction time(s). (s)**
K-C-UA	16.53	1760	K-C-UB	36.60	795	K-C-US	92.37	315
Na-C-UA	20.28	1435	Na-C-UB	20.78	1400	Na-C-US	66.13	440
NH-C-UA	34.43	845	NH-C-UB	77.59	375	NH-C-US	64.66	450
K-V-UA	149.22	195	K-V-UB	153.14	190	K-V-US	149.22	195
Na-V-UA	116.39	250	Na-V-UB	102.10	285	Na-V-US	132.26	220
NH-V-UA	100.34	290	NH-V-UB	93.86	310	NH-V-US	176.35	165

Upon completion of the NR calculation, the final pH value of the solution was determined to be 7.50.

Compared to a standard carbonation reactor, the NR was significantly improved when using venturi tubes for the carbonation zone. The NR of calcium carbonate obtained with the use of a venturi tube was 116.39 mol/s for Na-V-UA, 102.10 mol/s for Na-V-UB, and 132.26 mol/s for Na-V-US. An increase in NR values is achieved in calcium carbonate particle production due to the ultrasonic probe's seamless integration with the venturi tube. This research found that ultrasonic to venturi tube reactors had the greatest NR values, followed by venturi tube reactors and then conventional reactors.

4-4 The Effect of Ultrasonic Treatment on the Properties of Calcium Carbonate Particles

After calcium carbonate particles were made using traditional tube and venturi reactors, they underwent a 2-minute ultrasonic treatment with 100% amplitude. Calcium carbonate particles were created in two ways, as shown in Figure 4: first, by reducing the CO2 content, and second, by subjecting the resulting particles to ultrasonic treatment.

Table S1 lists the d10, d50, d90, and SPAN factor for calcium carbonate particles. Calcium carbonate particles obtained without ultrasonic treatment exhibited an unodal particle size distribution with a peak value bigger than 9 m, which corresponded to the d50 values of each particle. As a result of the cavitation effect, calcium carbonate cluster crystals are broken up into smaller particles during ultrasonic treatment, resulting in a twinned particle size distribution and a smaller average particle size (d50) of the final product. Studies have shown comparable behaviour, with one study claiming that using ultrasonic treatment led to obtaining vaterite crystals with lower particle sizes. Under these conditions, the d50 value of calcium carbonate particles in the presence of K+ ions was 4.83 m for the traditional reactor and 4.55 m for the venturi tube reactor. The d50 value of calcium carbonate particles was calculated to be 5.44 micrometres in the presence of Na + ions when using a traditional tube reactor and 4.64 micrometres when using a venturi tube reactor. The calcium carbonate particles used in the traditional tube and venturi tube reactors had

d50 values of 11.20 and 8.87 µm, respectively, when they were produced in the presence of NH4+ ions.

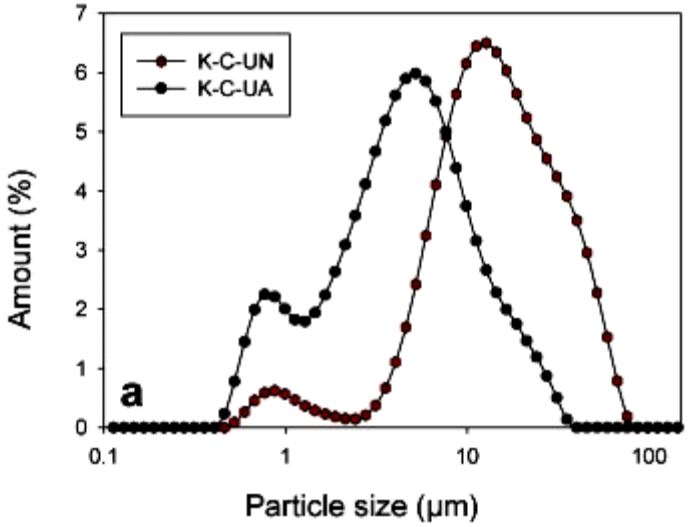

Figure 7-4 particle size distribution of calcium carbonate particles produced under KC-UN and KC-UA conditions.

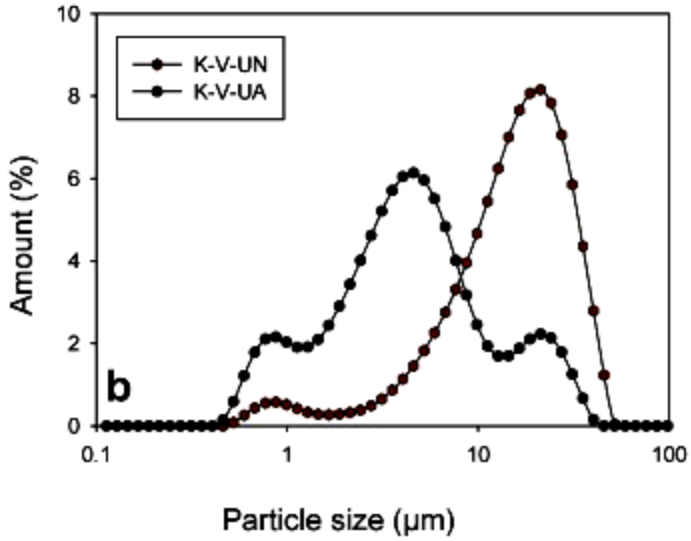

Figure 8-4 Particle size distribution of calcium carbonate particles produced under Na-C-UN and Na-C-UA conditions

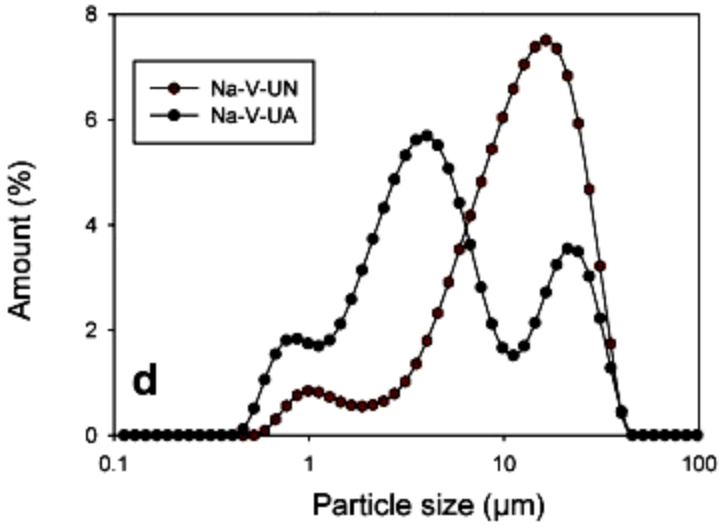

Figure 9-4 Particle size distribution of calcium carbonate particles produced under NH-C-UN conditions

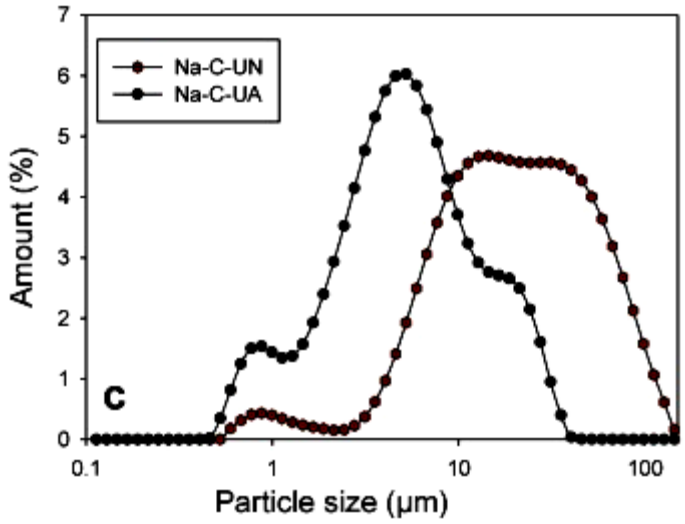

Figure 10-4 Particle size distribution of calcium carbonate particles produced under NH-C-UA conditions

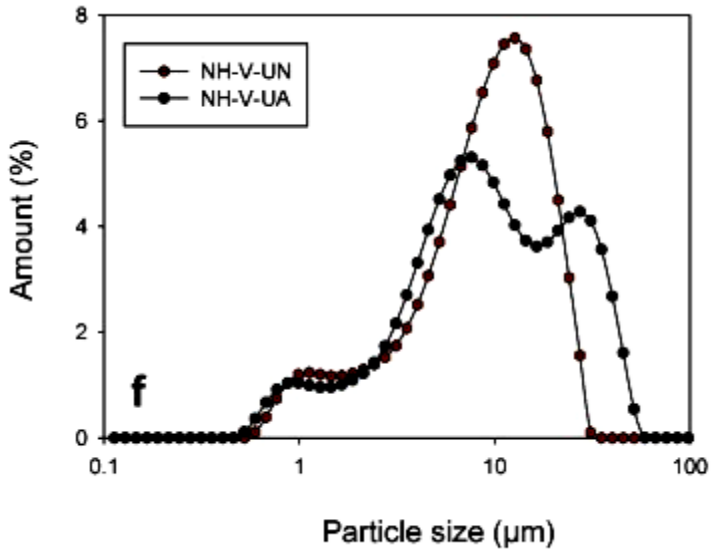

Figure 11-4 Particle size distribution of calcium carbonate particles produced under Na-V-UN and Na-V-UA

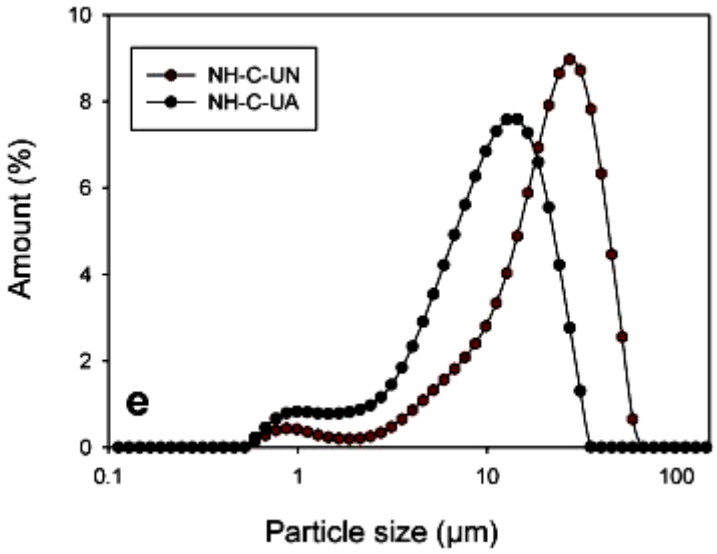

Figure 12-4 Particle size distribution of calcium carbonate particles produced under NH-V-UN and NH-V-UA.

X-ray diffraction analysis was used to establish the particles' polymorphism when calcium carbonate was synthesised (Figure 5). The polymorphism characteristics of calcium carbonate particles were found to be unaffected by the different reactor configurations. Results from both the

standard reactor and the venturi tube reactor were equivalent. All calcium carbonate particles with sharp peaks corresponding to calcite crystals were obtained in an XRD analysis in the presence of K and Na + ions (Exp. code: KC-UN, Na-C-UN, KV-UN and Na-V -UN), while a mixture of calcite and vaterite crystals was obtained in calcium carbonate particles as NH4 ions and has led to the production of vaterite crystals.

The impact of ultrasonic treatment on calcium carbonate particles' polymorphic characteristics has been the subject of a lot of research. The most stable form of CaCO3 in the environment, calcite crystals have been formed by ultrasonicating vaterite, a mineral that is prone to crystallisation. When the ultrasonic approach was applied in this investigation, no change was seen in the polymorphic features of all the calcium carbonate particles generated. After sonication, calcite crystals were detected in calcium carbonate particles under KC-UA, Na-C-UA, KV-UA and Na-V-UA circumstances, while the mixture of calcite and vaterite in calcium carbonate particles was determined for testing in NH-C-UA and NH-V-UA settings. According to Rietveld analysis (Table S2), ultrasonic treatment increased the percentage of calcite and vaterite in calcium carbonate particles, but no polymorphic alterations were seen in particles with NH4+ ions. The fraction of calcite crystals in the generated calcium carbonate particles was determined to be 53.64% under NH-C-UN circumstances. Calcium carbonate particle calcite crystal content increased to 56.44 percent after two minutes of ultrasonic treatment at maximum amplitude (source code: NH-C-UA). Similar results have been observed in calcium carbonate particles produced using a venturi tube (Exp code: NH-V-UN and NH-V-UA) (Exp code: NH-V-UN and NH-V-UA). These results are at odds with those of a recent study that found that ultrasonic treatment enhanced the percentage of vaterite crystals.

Chapter Five: Conclusion and Recommendations

5-1 Discussion and conclusion

The effect of ultrasonic application in the carbonation method's production of calcium carbonate particles from gypsum waste was examined in this study using three reactors (conventional, venturi tube, and venturi tube with an ultrasonic probe) in the presence of different alkaline sources (NaOH, KOH, and NH4OH). To determine the precise impact of ultrasonic application on the characteristics of calcium carbonate particles, it has been applied three times (before, during, and after calcium carbonate formation). SEM, XRD, AFM, SSA, FTIR, and particle size analyses were all used to examine the manufactured calcium carbonate particles. The following is a ranking of reactor types based on the nucleation time needed to create calcium carbonate: In order of decreasing length, we have: I a venturi tube equipped with an ultrasonic probe; (ii) a venturi tube; and (iii) conventionalreactors.

Ultrasonic processing had a substantial effect on the particle size distribution of all the products. In the presence of Na + or K + ions, every calcium carbonate particle was positively identified as calcite, while NH4 ions resulted in a mixture of vaterite and calcite crystals. In addition, it has been observed that the employment of ultrasonic power during the manufacture of calcium carbonate leads to the creation of single calcite crystals instead of a mixture (calcite and vaterite) in the presence of NH4 ions.

Calcium carbonate particles with improved features, such as a higher SSA value, uniform particle size, and nano-sized crystal qualities, were produced by using ultrasonic power before beginning the CO2 gas flow to the venturi tube reactor. Finally, depending on the production conditions, the calcium carbonate particles created in this study can be employed as fillers in many industrial domains, such as paints, paper, and plastics. The chemical and fertiliser industries can assess the solution's value once it has been used to produce calcium carbonate.

References

1. Shabab Saad, Harsovin Kaur, Giovanniantonio Natale. Scalable Chemical Synthesis Route to Manufacture pH-Responsive Janus CaCO3 Micromotors. Langmuir 2020, 36 (42) , 12590-12600. https://doi.org/10.1021/acs.langmuir.0c02148
2. Dan Wang, Cang Xiong, Wenzheng Li, Jun Chang. Growth of Calcium Carbonate Induced by Accelerated Carbonation of Tricalcium Silicate. ACS Sustainable Chemistry & Engineering 2020, 8 (39) , 14718-14731. https://doi.org/10.1021/acssuschemeng.0c02260
3. Mikhail V. Zyuzin, Dmitrii Antuganov, Yana V. Tarakanchikova, Timofey E. Karpov, Tatiana V. Mashel, Elena N. Gerasimova, Oleksii O. Peltek, Nominé Alexandre, Stéphanie Bruyere, Yulia A. Kondratenko, Albert R. Muslimov, Alexander S. Timin. Radiolabeling Strategies of Micron- and Submicron-Sized Core–Shell Carriers for In Vivo Studies. ACS Applied Materials & Interfaces 2020, 12 (28) , 31137-31147.
4. Addadi L, Raz S, Weiner S (2003) Taking advantage of disorder: amorphous calcium carbonate and its roles in biomineralization. Adv Mater 15(12):959–970
5. Ajikumar PK, Wong LG, Subramanyam G, Lakshminarayanan R, Valiyaveettil S (2005) Synthesis and characterization of monodispersed spheres of amorphous calcium carbonate and calcite spherules. Cryst Growth Des 5(3):1129–1134
6. Barhoum A, Van Assche G, Makhlouf ASH, Terryn H, Baert K, Delplancke M-P, El-Sheikh SM, Rahier H (2015a) A green, simple chemical route for the synthesis of pure nanocalcite crystals. Cryst Growth Des 15(2):573–580
7. Chen Z, Nan Z (2011) Controlling the polymorph and morphology of CaCO3 crystals using surfactant mixtures. J Colloid Interface Sci 358(2):416–422
8. Cölfen H (2003) Precipitation of carbonates: recent progress in controlled production of complex shapes. Curr Opin Colloid Interface Sci 8(1):23–31
9. D'Haese M, Langouche F, Van Puyvelde P (2013) On the effect of particle size, shape, concentration, and aggregation on the flow-induced crystallization of polymers. Macromolecules 46(9):3425–3434
10. Deng Y, Yoon S, Ragauskas A, White D (2008) Methods and compositions for papermaking. Pat. Apl. No. 2008/087396 A1, US Patent Office
11. Domingo C, López AM, Fraile J, Hidalgob A (2015) Supercritical CO2 for the reactive precipitation of calcium carbonate: uses and applications to industrial processing:

supercritical fluid nanotechnology. Advances and applications in composites and hybrid nanomaterials, p 233

12. El-Sherbiny S, El-Sheikh S, Barhoum A (2015) Preparation and modification of nano calcium carbonate filler from waste marble dust and commercial limestone for papermaking wet end application. Powder Technol 279:290–300
13. Feng B, Yong AK, An H (2007) Effect of various factors on the particle size of calcium carbonate formed in a precipitation process. Mater Sci Eng A 445–446:170–179
14. Hassas BV, Karakaş F, Çelik M (2013) Substitution of TiO2 with PCC (precipitated calcium carbonate) in waterborne paints. In Proceedings international mining congress and exhibition of turkey (IMCET2013).
15. Kuusisto, J., Tiittanen, T., and Maloney, T., (2016). Property optimization of calcium carbonate precipitated in a high shear, circulation reactor, Powder Technology 303, 241-250.
16. Asadi khansari, R., Dehghani Firouzabadi, m., and Resalati, H., (2017). The effect of coatings and coating weight by two types of PCC on barrier and optical properties and roughness of paper. Iranian Journal of Wood and Paper Industries, 8(2): 283-295(In Persian).
17. Manghuli, M.T. Asadpur Atoei, Gh., Nazarnezhad, N., and Zabih Zadeh, S.M., (2016). The influence of type of calcium carbonate fillers on the performance AKD and mechanical properties of printing and writing paper. Iranian Journal of Wood and Paper Industries, 7(1): 69-77. (In Persian).
18. Knez, S., Klinar, D., and Golob, J., (2006). Stabilization of PCC dispersions prepared directly in the motherliquid after synthesis through the carbonation of (hydrated) lime. Chemical Engineering Science 61, 5867– 5880.
19. Zhao, Y.L., Hu, Z.S., Ragauskas, A.J., and Deng, Y., (2005). Improvement of paper properties using starchmodified precipitated calcium carbonate filler. Tappi Journal 4(2), 3–7.
20. Mo Jung, W., Hoon Kang, S., Kim, W.-S., and Kyun Choi, C., (2000). Particle morphology of calcium carbonate precipitated by gas-liquid reaction in a Couette-Taylor reactor. Chemical Engineering Science 55, 733-747.

21. Declet, A., Reyes, E., and Suárez, O.M., (2016). Calcium carbonate precipitation: A review of the carbonate crystallization process and applications in bioinspired composites. Reviews on Advanced Materials Science 44, 87-107.
22. Montes-Hernandez, G., Renard, F., Geoffroy, N., Charlet, L., and Pironon, J.,(2007). Calcite Precipitation from CO2–H2O–Ca (OH)2 Slurry under High Pressure of CO2. Journal of Crystal Growth 308, 228-236.
23. Saraya, M.E.I., and Rokbaa, H.H.A.L., (2016). Preparation of vaterite calcium carbonate in the form of spherical nano-size particles with the aid of polycarboxylate superplasticizer as a capping agent. Am J Nano 4(2), 44–51.
24. Kuusisto, J.E., and Maloney, T.C., (2015). The effect of carbonation on the properties of carbohydrate-calciun carbonate hybrid pigments. BioResources, 10(2), 3277-3292.
25. Yang, H., Qiu, L., Qian, X., and Shen, J.,(2013). Filler modification for papermaking with cationic starch and carboxymethyl cellulose: A comparative study. BioResources 8(4), 5449-5460.
26. Antunes, E., Garcia, F.A.P., and Ferreira, P., (2008). Use of new branched cationic polyacrylamides to improve retention and drainage in papermaking. Ind. Eng. Chem. Res. 47, 9370-9375.
27. Chauhan, V.S., and Bhardwaj, N.K., (2014). Cationic starch preflocculated filler for improvement in filler bondability and composite tensile index of paper. Industrial & Engineering Chemistry Research 53(29), 11622-11628.
28. Sang, Y., McQuaid, M., and Englezos, P., (2011). Pre-flocculation of precipitated calcium carbonate filler by cationic starch for highly filled mechanical grade paper. BioResources 7(1), 0354-0373.
29. Boudali, A. Abada, M. Driss Khodja, B. Amrani, K. Amara, F. Driss Khodja, A. Elias, *Physica B*, **405**, 2010, 3879.
30. X. Jiang, M.A. Trunov, M. Schoenitz, R.N. Dave, E.L. Dreizin,(2009), Journal of Alloys and Compounds, **478**, 2009, 246.
31. V.V. Lemanov, A.V. Sotnikov, E.P. Smirnova, M. Weihnacht, R. Kunze,(1999), Solid State Communications, **110**, 1999, 611.
32. S.G. Javed, A. Khan, A. Majid, A.M. Mirza, J. Bashir,(2007), Computational Materials Science, **39**, 2007, 627.

33. Y. Saito, H. Takao, K. Wada,(2008), Ceramics International, **34**, 2008, 745.
34. M.L. Moreira, E.C. Paris, G.S. Nascimento, V.M. Longo, J.R. Sambrano, V.R. Mastelaro, M.I. Bernardi, J. Andres, J.A. Varela, E.(2009), Longo, Acta Mater., **57**, 2009, 5174.
35. K.T. Jacob, K.P. Abraham, J. Chem.(2009), Thermodynamics, **41**, 2009, 816.
36. S.K. Manik, S.K. Pradhan, M. Pal, Physica E, **25**, 2005, 421.
37. X. Wu, Y. Dong, S. Qin, M. Abbas, Z. Wu,(2005), Solid State Communications, **136**, 2005, 416.
38. L. Taibi, A. Mezroua, R.(2004), von der Muhll, Solid State Chem., **124**, 2004, 77.
39. B.M. Patil, R.S. Srinivasa, S.R.(2007), Dharwadkar, Bull. Mater. Sci., **30**, 2007, 225.
40. W. Liu, C. Wang, J. Cui, Z. Yong Man,(2009), Solid State Communications, **149**, 2009, 1871.
41. P. Hu, H. Jiao, C. Hai Wang, X. Ming Wang, S. Ye, X.P. Jing, F. Zhao, Z.X. Yue, (2011), Materials Science and Engineering B, **176**, 2011, 401.
42. L.S. Cavalcantea, V.S. Marques, J.C. Sczancoski, M.T. Escote, J.A. Varela, M.R. Santos, P.S. Pizani, E. Longo,(2008), Chemical Engineering Journal, **143**, 2008, 299.
43. V.S. Marques, L.S. Cavalcante, J.C. Sczancoski, D.P. Volanti, J.W. Espinosa, M.R. Joya, M.R. Santos, P.S. Pizani, J.A. Varela, E. Longo,(2008), Solid State Sciences, **10**, 2008, 1056.
44. S. Palaniandy, N. Hidayu Jamil,(2009), Journal of Alloys and Compounds, **476**, 2009, 894.
45. G. Mi, F. Saito, Sh. Suzuki, Y. Waseda,(1998), Powder Technology, **97**, 1998, 178.
46. S.K. Manik, S.K. Pradhan,(2004), Materials Chemistry and Physics, **86**, 2004, 284.
47. C. Suryanarayana,(2001), Progress in Materials Science, **46**, 2001, 1.
48. J. Wang,(2007), Materials Letters, **61**, 2007, 4393.
49. Z. Liu, K.C. Chan, L. Liu, S.F. Guo,(2012), Materials Letters, **82**, 2012, 67.
50. C. Dwivedi, N. Raje, J. Nuwad, M. Kumar, P.N Bajaj, (2012), Chemical Engineering Journal, **193**, 2012, 178.
51. M.G. Ha, M.R. Byeon, T.E. Hong, J.S. Bae, Y. Kim, S. Park, H. Soon Yang, K.S. Hong,(2012), Ceramics International, **38**, 2012, 1365.
52. Z. Song, Y. Cheng, J. Guo, J. Wu, G. Xu, P. Cui,(2012), Colloids and Surfaces A: Physicochemical and Engineering Aspects, **396**, 2012, 305.

53. C.Y. Chen, K. Ozasa, K. Katsumata, M. Maeda, K. Okada, N. Matsushita, (2012),Electrochemistry Communications, **22**, 2012, 101.
54. H. Zhang, G. Chen, X. He, J. Xu,(2012), Journal of Alloys and Compounds, **516**, 2012, 91.
55. D. Zhang, C. Zhang, P. Zhou,(2011), Journal of Hazardous Materials, **186**, 2011, 971.
56. C. Ergun, (2011), Ceramics International, **37**, 2011, 1143.
57. Y. Boyjoo, V. K. Pareek and J. Liu,(2014), Synthesis of micro and nano-sized calcium carbonate particles and their applications. Journal of Materials Chemistry A, Vol. 2, pp. 14270-14288 (2014)
58. N. G. M. Palmqvist,(2017), "Nanoparticles: Case studies of their synthesis, properties and biological interaction," in Department of Molecular Sciences, Ed., Swedish University of Agricultural Sciences, 2017.
59. Z. Hu, Y. Deng and Q. Sun,(2004), Synthesis of precipitated calcium carbonate nanoparticles using a two-membrane sySEM. Colloid Journal, Vol. 66, pp. 745-750 (2004)
60. F. Guo, Y. Li, H.-X. Xu, G.-Q. Zhao and X.-J. He,(2007), Size-controllable synthesis of calcium carbonate nanoparticles using aqueous foam films as templates. Materials Letters, Vol. 61, pp. 4937-4939 (2007)
61. M. Huber, W. J. Stark, S. Loher, M. Maciejewski, F. Krumeich and A. Baiker, (2005), Flame synthesis of calcium carbonate nanoparticles. Chemical Communications, pp. 648-650 (2005)
62. S. Biradar, P. Ravichandran, R. Gopikrishnan, V. Goornavar, J. C. Hall, V. Ramesh, S. Baluchamy, R. B. Jeffers and G. T. Ramesh, (2011), Calcium carbonate nanoparticles: synthesis, characterization and biocompatibility. Journal of Nanoscience and Nanotechnology, Vol. 11, pp. 6868-6874 (2011)
63. J. Sargheini, A. Ataie, S. Salili and A.(2012), Hoseinion, One-step facile synthesis of CaCO3 nanoparticles via mechano-chemical route. Powder technology, Vol. 219, pp. 72-77 (2012)
64. Suster, H; Arabic, e; Shah Tahmasabi, N; Javadi, M. (2014), Synthesis and investigation of structural and optical properties of calcium hydroxide nanoparticles by sonochemical method, Proceedings of the 12th Condensed Matter Conference of the Iranian Physics Association, Isfahan University of Technology, 8th and 9th of Bahman.

65. Nanni, A. and Dei, L.,(2003), "Ca(OH)2 nanoparticles from W/O microemulsions", Langmuir, vol. 19, no. 3, pp. 933-938, 2003.
66. Ghafouri Najafabadi, F; Saraf Mamori, R; Riahi Nouri, N., (2012), simultaneous synthesis of ceria and magnesia nano powders by chemical method, master's thesis in materials engineering, technical and engineering faculty, Tarbiat Modares University.
67. G. Walton and H. Füredi,(1979), "The formation and properties of precipitates", RE Krieger Publishing Co., pp. 28-120, 1979.
68. S. Hamada, Y.Kudo, and K. Mingawa,(1990), "The formation of mono dispersed indium (III) hydroxide particles by forced hydrolysis at elevated temperature", J. Bulletin of Chemical Society of Japan, Vol 63, pp 102-107, 1990.
69. S. J. Pennycook, A. R. Lupini, M. Varela, A. Y. Borisevich, Y. Peng, M. P. Oxley, K. van Benthem and M. F.(2007). Chisholm, Scanning Transmission Electron Microscopy for Nanostructure Characterization, first ed., Springer.
70. R.F. Egerton,(2009), Rep. Prog. Phys.,72, 1-25.
71. H. Daniels, A. Brown, A. Scott,(2003), Ultramicroscopy,96, 523-534.
72. N. Tanaka and K. Saitoh,(2014), Basics of STEM. Scanning Transmission Electron Microscopy of Nanomaterials, first ed.,Imperial College Press.
73. D.T. Nguyen, S.D. Findlay, and J. Etheridge,(2014), Ultramicroscopy,146, 6-16.
74. G.T. Martinez, A. Rosenauer, A. De Backer,(2014), Ultramicroscopy,137, 12-19.
75. G.T. Martinez, A. Rosenauer, A. De Backer, (2014), Micron,63, 57-63.
76. X. Sang, and J.M. LeBeau,(2014), Ultramicroscopy,138, 28-35.
77. F. Krumeich, E. MUller, and R.A. Wepf, (2013), Micron,49, 1-14
78. S.D. Findlay, Y. Kohno, L. A. Cardamone,(2014), Ultramicroscopy,136, 31-41.
79. S.D. Findlay, N. Shibata, H. Sawada, E, Okunishi, Y. Kondo, Ultramicroscopy,110 (2010) 903-923.
80. S.D. Findlay, N. R. Lugg, N. Shibata, L. J. Allen, and Y. Ikuhara,(2011), Ultramicroscopy,11, 1144-1154.
81. K. Kimoto,T. Asaka, X. Yu, T. Nagai,(2010), Ultramicroscopy,110, 778-782.
82. Kaufmann, Elton N.(2003), "Characterization of Materials, 2 Volume Set." *Characterization of Materials, 2 Volume Set, by Elton N. Kaufmann (Editor), pp. 1392. ISBN 0-471-26882-8. Wiley-VCH, January 2003.*

83. Goldstein, Joseph I., et al.(2017), *Scanning electron microscopy and X-ray microanalysis*. Springer, 2017.
84. http://en.wikipedia.org/wiki/Scanning_electron_microscope
85. Goodhew, P. J., Humphreys, J., Beanland, R.,(2001), "Electron Microscopy and Analysis", 3rd Edition. London: Taylor & Francis.
86. Zhou, W., Wang, Z. L. (Editors),(2006), "Scanning Microscopy for Nanotechnology - Techniques and Applications", New York: Springer.
87. http://www.microscopemaster.com/scanning-electron-microscope.html
88. Goldstein, J. I., Newbury, D., Joy, D. C., Lyman, C. E., Echlin, P., Lifshin, E., Sawyer, L., Michael, J. R.,(2003), "Scanning Electron Microscopy and X-Ray Microanalysis", 3rd Edition. New York: Kluwer Academic/Plenum.
89. H. Yurdakul, J. C. Idrobo, S. J. Pennycook,(2011), Scripta Materialia, 65, 656-659.

ISLAMIC AZAD UNIVERSITY

MASHHAD BRANCH

Faculty of Engineering

Thesis for receiving (M.SC) degree on Metallurgy and Ceramic Engineering

Subject:

Synthesis Nono Calcium Carbonate from Waste Gypsum

Supervisor:

Ebrahim Zohourvahid-Karimi Ph.D.

By:

2022